Methane Distribution, Fluxes, and Budget in the East China Sea and Yellow Sea

M.-S. Sun [1,2,*], G.-L. Zhang[1,2], X.-P. Cao[1], X.-Y. Mao[3], J. Li[4], W.-W. Ye[1]

[1]{Key Laboratory of Marine Chemistry Theory and Technology, Ministry of Education, Ocean University of China, Qingdao 266100, P R China}

[2]{Qingdao Collaborative Innovation Center of Marine Science and Technology, Ocean University of China, Qingdao 266100, P R China}

[3]{College of Physical and Environmental Oceanography, Ocean University of China, Qingdao 266100, P R China}

[4]{State Key Laboratory of Satellite Ocean Environment Dynamics, Second Institute of Oceanography, State Oceanic Administration, Hangzhou 310012, P R China}

[*]{Present address: Helmholtz Center for Ocean Research Kiel (GEOMAR), 24105 Kiel, Germany}

Correspondence to: G.-L. Zhang (guilingzhang@ouc.edu.cn)

Abstract

We measured dissolved methane (CH_4) concentrations, saturations, and air-sea fluxes and sediment-water fluxes during five cruises in March, May, August, October, and December of 2011 in the East China Sea (ECS) and the Yellow Sea (YS). CH_4 concentrations had obvious spatial and seasonal variability due to the complex mixing of different water masses and other variables. Maximum CH_4 concentration, sea-air and sediment-water fluxes all occurred during summer. CH_4 concentration decreased gradually from the coastal area to the open sea, and high levels of CH_4 generally appeared near the Changjiang Estuary and outside the Hangzhou Bay. In early spring and winter, CH_4 in the shelf region had a uniform distribution from the surface to the bottom, while it increased gradually with depth in other seasons. Subsurface CH_4 maximum occurred at a depth of about 200 m in the slope region during May, October, and December. The CH_4 levels at the bottom were generally higher than at the surface, and this was enhanced during summer due to the occurrence of hypoxia in the bottom waters. Changjiang Diluted Water, Kuroshio, and Taiwan Warm Current Water affected the geographic distribution of CH_4 in the ECS, and these water bodies contributed about 3.45, 2.97, 14.60 $mol \cdot s^{-1}$ of CH_4 to the ECS during summer and 2.11, 5.28, 5.20 $mol \cdot s^{-1}$ CH_4 during winter, respectively. Sediment was also a significant source of dissolved CH_4 in the ECS, and we estimated the average sediment-water CH_4 flux of the ECS and YS as about 1.06 and 0.73 $\mu mol \cdot m^{-2} \cdot d^{-1}$, respectively. We used a box model to calculate preliminarily the CH_4 budget in the ECS, which suggests that the main CH_4 sources in the ECS were *in situ* CH_4 formation in water column and sediment emissions. Air-sea exchange was the major external sink of CH_4 in the ECS. We estimated total annual CH_4 emission from the ECS and YS to be about 4.09×10^9 mol/yr, hence the ECS and YS are active areas for CH_4 production and emission.

1 Introduction

Methane (CH_4) is an active atmospheric trace gas that is responsible for about 23% of the global greenhouse effect, and also participates in atmospheric chemistry and the biogeochemical cycle of global carbon (Crutzen and Zimmermann, 1991; Quay et al., 1999; IPCC, 2013). The global atmospheric CH_4 has increased significantly since the industrial revolution, and was reported as 1803±2 ppb in 2011, which is about 2.5-fold higher than that (722±25 ppb) in 1750 (IPCC, 2013). The continuing rise of atmospheric CH_4 indicates an imbalance of sources and sinks. Natural sources are responsible for about 40% of global CH_4 emission (Shakhova et al., 2010), among which the ocean accounts for only about 0.4-5.0% of the total emission (Crutzen, 1991; Bange et al., 1994; Reeburgh, 2007). Although most of oceanic CH_4 are oxidized by O_2 and sulfate in both aerobic and anaerobic environment before emission, ocean still releases about 11-18 Tg CH_4 yr^{-1} (Bange et al., 1994) into the air. In marine ecosystems, CH_4 distributions and emissions have large spatial and temporal variations (Bange et al., 1994, 2004; Kock et al., 2008; Forster et al., 2009; Zhang et al., 2004, 2008a). Shelf areas and estuaries were estimated to contribute about 75% to the global oceanic CH_4 emissions, although they just cover a small part of the world´s oceans (Bange et al., 1994). However, this estimate still has great uncertainties due to large spatial and seasonal variations and limited area coverage.

The East China Sea (ECS) and the Yellow Sea (YS) together forms an important marginal sea of the northwestern Pacific Ocean. This is one of the largest continental shelves in the world, with a total surface area of 1.2×10^6 km^2. The ECS opens its north to the YS with the straight line from the northern tip of the mouth of the Changjiang (Yangtze River) toward the Jeju Island as the boundary (the blue dashed line in Fig. 1). The ECS stretches south to the Taiwan Strait, and is adjacent to the western Pacific along its east edge. Its total area is about 7.7×10^5 km^2, and the average water depth is about 72 m. This wide and river-dominated shelf receives large amounts of fresh water (9.03×10^{11} $m^3\cdot year^{-1}$), sediment (4.14×10^8 $t\cdot year^{-1}$) (Wang et al., 2008), and nutrients (Zhang et al., 1996; Gao et al., 2012) from the Changjiang. The hydrographic characters of this region are also influenced greatly by a circulation system including the Kuroshio, Tsushima Warm Current, Yellow Sea Warm Current on the eastern boundary of the shelf, the Coastal Currents along the western side and the Taiwan Warm Current dispersing out in the middle shelf (Su, 1998; Zhang et al., 2007; Yuan et al., 2008).

So far oceanic CH_4 emission is poorly quantified, owing to lack of the temporal continuity and areas coverage (Bange et al., 2009). In particular, data on CH_4 in coastal areas of China are scattered and fragmentary. In early 1990s, Tsurushima et al. (1996) observed the horizontal and vertical distribution of CH_4 along the section “PN line” in the ECS. Rehder and Suess (2001) surveyed the distribution of CH_4 in surface waters along the main path of Kuroshio, which only covered a small part of areas in the East China and South China Sea. Zhang et al. (2004) reported distributions and fluxes of CH_4 in the ECS and the YS in spring 2001, and they also estimated CH_4 input from the Changjiang and CH_4 export from the shelf to Kuroshio water. Yang et al. (2010) reported the seasonal variation of CH_4 concentrations and air-sea fluxes in the north YS during 2006 and 2007. Ye et al. (2015) and Zhang et al. (2008a) reported CH_4 distributions and fluxes in the ECS in summer, but the former emphasized the influence of hypoxia on CH_4 distribution in the bottom water, while the later mainly introduced the high spatial variability of CH_4 depth profiles along four sections. Although these results give us a glimpse of CH_4 in coastal waters of China, they are still far from understanding the seasonal variations of CH_4 distribution and emission, and quantifying CH_4 sources and sinks in these areas. Thus more data on CH_4 in coastal and shelf waters of China are still needed to further enrich the global oceanic CH_4 database, and to understand the biogeochemical cycle of CH_4 in the shelf areas and their regional contribution to global oceanic CH_4 emission.

In this paper, we characterized the spatial distribution and seasonal variation of dissolved CH_4 in the ECS and YS based on data collected during five cruises in 2011, and identified factors that affected these patterns. We also estimated fluxes at the sea-air and sediment-water interfaces to determine the amount of CH_4 released by the ECS into the atmosphere and the amount that escaping from sediments into the water column. We used a box model to calculate the preliminary CH_4 budget in the ECS, identify the main sources and sinks of dissolved CH_4 in this area, and estimate the contribution of different sources to CH_4 in ECS quantitatively. The ultimate aims of this research are to provide a deep understanding of dissolved CH_4 in the ECS, and to improve our knowledge of CH_4 cycle in the shelf region.

2 Materials and methods

2.1 Seawater sampling and analysis

Five cruises were conducted in the ECS and YS during 2011 to collect data at different locations (Fig. 1, Table 1). Seawater samples were collected at different depths using 5-L or 8-L Niskin bottles mounted to a Sea-Bird CTD rosette. Surface waters were collected at a depth of ~2 m, and bottom waters were typically collected at ~3 m above the seafloor. Two subsamples for CH_4 determinations were transferred from the Niskin bottles into glass vials (~117 mL) using a silicone tube. After overflow of approximately 1.5- to 2-fold of bottle volume, 1 mL of a saturated solution of $HgCl_2$ was added to inhibit microbial activity. Then, the sample bottle was immediately sealed with a butyl rubber stopper and an aluminum cap (to exclude excess water) and stored upside down in a dark box (Zhang et al., 2008a). All water samples were analyzed after return to the laboratory, within 60 days after collection (Zhang et al., 2004). Salinity and temperature data were measured by the CTD, and oxygen data from CTD profiles were calibrated with oxygen measurements from the Winkler titration method (Bryan et al., 1976). Wind speeds were measured by the shipboard automatic weather stations at about 10 m above the sea surface.

Dissolved CH_4 from seawater samples was measured using a gas-stripping method and a GC-14B gas chromatograph (Shimadzu, Japan) with a flame ionization detector (FID) (Zhang et al., 2004). FID responses were calibrated using known volumes of CH_4 standards (2.02, 4.18, and 50.0 ppmv, Research Institute of China National Standard Materials). There was a linear relationship between FID response and CH_4 concentration, so a multi-point calibration method was used to determine CH_4 concentration based on chromatographic peak area. The precision of this method was better than 3% during the routine analysis of the seawater samples (Zhang et al., 2004).

2.2 Sediment sampling and incubation experiments

The emission of CH_4 from sediments was measured by the closed chamber incubation method (Barnes and Owens, 1999). Sediment samples were collected by a box corer at different sampling stations (Fig. 1, red triangles). Only samples with undisturbed sediment surfaces were used. At each station, 15 sediment cores were collected using plexiglass tubes that had openings on both ends (i.d.= 5 cm, height =

30 cm), with the bottoms sealed using air-tight rubber bungs. Just prior to the beginning of flux measurements, ambient bottom water was added carefully (with no gas headspace), and then the core was capped with a plexiglass top that had gas-tight O-ring seals and two sampling ports. All cores were arranged around a central shaft which was supported by magnets that rotated at 60 rpm, and were placed in a water-filled tank that was held at ambient room temperature using a recirculating water temperature-controlled bath. Ten glass bottles filled with ambient bottom water were placed in the same tank and used as blank. Cores were incubated in the dark for 24~48 h. Three overlying water samples were collected at 4-h to 8-h intervals, transferred into 56.5 mL glass bottles, and treated with 0.5 mL $HgCl_2$ to inhibit microbial activity. At the same time, two bottled water samples were also treated with 0.5 mL $HgCl_2$ as a blank. The CH_4 concentrations of all samples were measured by the gas-stripping method described above. Sediment-water CH_4 flux was estimated from the slope of the CH_4 increase in the overlying water as a function of time. The effect of temperature discrepancy (usually 0.8-10.5ºC) on the CH_4 emission rate from sediments was corrected by the Arrhenius empirical equation (Aller et al., 1985; Song et al., 2015). When temperature increases by 10 °C, the chemical reaction rate (here referring to CH_4 production and consumption rate) will increase by 2~4 times. We took 3 times for calibrating the calculation of sediment-water CH_4 fluxes accordingly. Use of the Arrhenius equation for temperature correction is usually reasonable and acceptable when an incubation experiment is not conducted at the *in situ* temperature (e.g. Aller et al., 1985; Song et al., 2015).

2.3 Saturation and sea-to-air flux calculations

The saturation (R, %) and sea-to-air flux (F, $\mu mol \cdot m^{-2} \cdot d^{-1}$) of CH_4 were calculated by the following formulas:

$$R\ (\%) = C_{obs} / C_{eq} \times 100 \qquad (1)$$

$$F = k \times (C_{obs} - C_{eq}) \qquad (2)$$

where C_{obs} is the observed concentration of dissolved CH_4 and C_{eq} is the air-equilibrated seawater CH_4 concentration, calculated from the *in situ* temperature and salinity and the solubility data of Wiesenburg and Guinasso (1979). Atmospheric CH_4 was not measured in this study. Instead, an annual mean atmospheric CH_4 mixing ratio of 1902 ppb at three observation stations near the East China Sea (LLN, TAP and SDZ) in 2011, from the NOAA/ESRL Global Monitoring Division in situ program (http://www.esrl.noaa.gov/gmd), was used for all calculations. Although seasonal variations in atmospheric CH_4 mixing ratios were detected in these stations due to terrestrial influence, they make a minor difference in the results of sea-air fluxes. In formula 2, *k* stands for the gas transfer coefficient, which is a function of wind speed and Schmidt number (Sc), generally estimated by the empirical equations. Various empirical equations were published to estimate *k*. Nightingale et al. (2000) reported an evaluation of sea-air gas exchange in coastal ocean, and the corresponding value lies near the median of extensive methods and models (Cockenpot et al., 2015). Wanninkhof (2014) improved the methodology and updated the relationship between gas exchange and wind speed based on his previous research over the last two decades (Wanninkhof, 1992). The new relationship between *k* and Sc was constructed using the modified global ocean ^{14}C inventories and improved wind speed products, and it can be well applied to the gas exchange study at the intermediate winds of 4-15 m/s. Both methods (hereafter N2000 and W2014) were chosen to calculate sea-air fluxes in this paper.

3 Results

3.1 Hydrography of the ECS

The hydrography of the ECS is highly variable due to the influence of three main water masses including the Changjiang Diluted Water, Taiwan Warm Current Water, and Kuroshio (Su, 1998; Li and Su, 2000; Zhang et al., 2007; Qi et al., 2014). These influences are evident in the temperature-salinity (T-S) curves along all sections during May, October, and December (Figs. 2 and 3). The salinities at stations near the Changjiang Estuary (*i.e.* C0, B1 in May; P01, F03 in October; F02, P01 in December) were less than 32, due to the influence of Changjiang Diluted Water (CDW). In contrast, the Kuroshio affected the T-S relationships at stations on the continental slope (*i.e.* CJ, D1, D9, ED and G8 in May; P12, E10 in October; E10 in December). Moreover, water columns of these stations could be divided into four layers according to their T-S relationships: *(i)* Kuroshio surface water (KSW) was present at a depth of 0~50 m, and this water had high temperature and salinity; *(ii)* Kuroshio subsurface water (KSSW) was at a depth of 50~300 m, and this water had a lower temperature than the surface water; *(iii)* Kuroshio intermediate water (KIW) was present at a depth of 300~800 m, and had lower salinity and temperature than the upper water; and *(iv)* Kuroshio deep water (KDW) was at 800 m and lower, and this high-density water had a temperature of about 5°C.

The Taiwan Warm Current Water (TWCW) also affected the mid-shelf of the ECS, as indicated by the high temperature and a moderate salinity 33.0~34.5 psu in the southwestern region of the ECS (stations T01, T03 in May; Z01, Z03 in October; Z02, Z03 in December). The shelf water mixed with water from the CDW, TWCW, KSW, and KSSW, and its salinity was 32~ 34 psu. High CH_4 levels were usually present in areas impacted by the CDW, and low CH_4 levels were present in the water from the Kuroshio Current.

3.2 Seasonal variations of CH_4 in the ECS and YS

Table 2 shows the range and average of temperature, salinity, and CH_4 concentrations in surface and bottom waters of the ECS and YS during the five cruises of 2011. Considering the large spatial difference among different cruises, we divided the sampling region into four subareas based on the boundary of the ECS and YS (blue dashed line in Fig. 1), the line of salinity 30 (green curve in Fig. 1) and the 200m depth line (red curve in Fig. 1). They were the YS, the Changjiang Estuary ($S \leq 30$), the ECS shelf ($S>30$, depth$\leq$200 m) and the ECS slope ($S>30$, depth>200 m). The ECS shelf was surveyed during all cruises and was chosen to compare the average surface and bottom CH_4 concentrations during different seasons (Fig. 4). It can be seen that both surface and bottom CH_4 concentrations had obvious seasonal variations, with the highest level occurring in summer and the lowest level in early spring (March). The salinity during August was the lowest due to the surge of Changjiang runoff in summer. CH_4 concentration in the Changjiang (135.3±36.9 nmol·L^{-1}) was usually about 10-30 times higher than that in the ECS, and this enhanced CH_4 concentration in the ECS together with high CH_4 production with increasing temperature. During the five cruises, bottom CH_4 concentrations were usually higher than those at the surface, especially during summer.

3.3 Geographic Distribution of CH_4 in the YS and ECS

Figure 3 shows the geographic distributions of temperature, salinity, and CH_4 in surface and bottom waters of the YS and ECS in 2011. Two cruises were in spring (March, Fig. 3a; May, Fig. 3b). During May, surface and bottom water temperature increased gradually from north to south, and temperature was relatively low (2~3°C) in the bottom water on the edge of the ECS continental shelf. Surface and bottom salinity increased gradually from the Changjiang Estuary to the southeast. Dissolved CH_4 concentrations in surface and bottom waters gradually declined from the Changjiang Estuary towards the open sea during spring. High CH_4 concentrations in the surface water appeared near Changjiang Estuary (T05: 29.67 nmol·L^{-1} in March; C0: 21.38 nmol·L^{-1} in May) due to the influence of the Changjiang Diluted Water. CH_4 concentrations in the bottom were slightly higher than in the surface, and highest levels were observed at F03 (30.63 nmol·L^{-1}) and F04 (19.58 nmol·L^{-1}) during March and at B1 (17.81 nmol·L^{-1}) and D1 (20.01 nmol·L^{-1}) during May. In the southeastern continental shelf of the ECS, CH_4 concentrations were relatively low (about 2~3 nmol·L^{-1}), mainly due to the influence of the CH_4-depleted Kuroshio surface water. This is consistent with the results reported by Rehder and Suess (2001) and Tsurushima et al. (1996).

Temperature in the surface and bottom waters increased from north to south during August (Fig. 3c). Salinity had a similar trend with spring, but CDW had an obvious extension in the ECS during summer, and surface salinity was below 32 at most regions of the continental shelf. Dissolved CH_4 increased with increasing temperature and freshwater discharge during summer (about 33,484 $m^3 \cdot s^{-1}$, more than 2-times than during spring; *Changjiang Sediment Bulletin*, 2011). The mean surface and bottom CH_4 concentrations were 8.21 $nmol \cdot L^{-1}$ and 11.88 $nmol \cdot L^{-1}$, respectively. Just as in spring, high CH_4 concentrations in the surface and bottom waters were present near the Changjiang Estuary and outside Hangzhou Bay. Particularly, high bottom CH_4 concentrations (10.51~12.48 $nmol \cdot L^{-1}$) were observed in the high turbidity zone of the Changjiang Estuary (~122°00′-122°20′E, 30°50′-31°15′N; Shen, 2012), together with low oxygen concentrations (2.10~2.82 $mg \cdot L^{-1}$). Besides, high temperature during summer may lead to water stratification, which prevents dissolved CH_4 in bottom waters from diffusing into upper waters, and thereby further enhance the CH_4 accumulation in the bottom water.

During October, surface seawater temperature and salinity increased gradually from northwest to southeast (Fig. 3d). Bottom temperatures in the ECS were almost all in the range of 19~22°C, but there was a cold bottom center (below 10°C) on the southeastern region of the YS. Water with high temperature and salinity at the southeastern corner of the studied area might have been affected by the northward branch of the Kuroshio. CH_4 concentrations during autumn were significantly lower than during summer. Bottom CH_4 concentrations of the entire ECS shelf were relatively high (above 8.0 $nmol \cdot L^{-1}$), especially at coastal areas, *i.e.* the Changjiang Estuary (P01, P03), the mouth of Hangzhou Bay (T05), and the surrounding waters of Jeju Island (A10, D07). On the contrary, CH_4 concentrations were quite low (about 3 $nmol \cdot L^{-1}$) in the southeastern part of the ECS continental shelf due to the influence of CH_4-depleted Kuroshio surface water.

The geographic distributions of surface and bottom temperature and salinity during December (Fig. 3e) were similar to that recorded during October, but CDW only had a slight influence. The CH_4 level of the whole ECS and YS during December was far below the levels during August and October, and the average CH_4 concentration in the surface waters (4.07 $nmol \cdot L^{-1}$) was slightly lower than that in the bottom waters (4.53

nmol·L^{-1}). Surface CH_4 concentrations in the YS were slightly higher than those in the ECS, and high CH_4 concentrations occurred in the southern YS near Cheju Island, while sporadically high levels of CH_4 in the bottom waters mainly occurred near the continental slope in the ECS. To sum up, CH_4 concentrations in the surface and bottom waters of the YS and ECS during winter were uniform and stable, and were 3~5 nmol·L^{-1} in most regions.

3.4 Depth Distribution of CH_4 in the ECS

Section PN (red solid line in Fig. 1) extends from the Changjiang Estuary southeast towards the Okinawa Trough and across the CDW and the mainstream of the Kuroshio. Section E (purple solid line in Fig. 1) lies across the entire shelf of the ECS, and extends from the coastal area of Zhejiang and Fujian provinces east towards the Okinawa Trough. We used these representative sections to study the hydrological and chemical characteristics of the ECS. Here we choose the top buoyant water (depth less than 200 m) to analyze the depth distribution of dissolved CH_4 on the ECS shelf.

Figure 5 shows the depth distributions of temperature, salinity, and CH_4 along section PN during March, May and October, and section E during December. Seawater temperature and salinity gradually increased with distance from the shore, but the depth profiles had seasonal variations. During early spring (March, Fig. 5a) and winter (December, Fig. 5d), the water column in the middle of ECS shelf was almost well-mixed in the top 100 m, and temperature and salinity along section PN were nearly uniform from the surface to the bottom; however, the depth profiles of temperature and salinity were stratified during late spring (May, Fig. 5b) and autumn (October, Fig. 5c). Perennial stratification in the water column occurred in the Changjiang Estuary, while water column stratification in the middle shelf began to occur during late spring, faded during the fall and disappeared completely during December.

Correspondingly, dissolved CH_4 concentrations along section PN and section E gradually decreased with distance from the shore, and the maximum CH_4

concentration of surface water was near the shore. During March and December, CH_4 concentrations were relatively uniform from surface to bottom, but they increased gradually with depth during May and October. Particularly, high bottom CH_4 values were usually observed at stations close to the continental shelf, especially in the shelf break area. The bottom CH_4 concentration at P09 during October reached 12.16 nmol·L^{-1}, almost 2-fold higher than the surface level.

Figure 6 shows depth profiles of seawater temperature, salinity, and CH_4 concentrations at stations CJ, P12, and E10 (red circles in Fig. 1) located at the continental slope where the mainstream of the Kuroshio flows northeastward along the 200 m isoline. The mixed layers at the sloping region ranged between 30 and 120 m in depth and became deeper from spring to winter, below the mixed layer water temperature decreased gradually. Salinity showed maximum at around 100-200 m, then declined sharply and reached minimum at about 500 m, below which a slight increase occurred with depth. All CH_4 concentrations increased initially with depth, and reached maximum at around 200 m, then decreased to yield a minimum at 500 m. The first CH_4 peak (3-6 nM) may be explained by advective supply from the adjacent continental slope, where bottom waters usually contain high levels of CH_4 (Ye et al., 2015). The second CH_4 peak occurred at a depth of 600 m during May and at 800 m during October. CH_4 concentrations further increased below 800 m during May and December, suggesting the existence of CH_4 sources in sediments.

3.5 Sediment-water CH_4 fluxes in the YS and ECS

Sediment-water fluxes of CH_4 from the ECS and YS had an obvious seasonal variation, with the maximum occurring in summer (Fig. 7) during which the flux was about 2-times higher than the other seasons. CH_4 was emitted from the sediments at most stations and acted as a net source of CH_4 in the water column. CH_4 release from sediments also had obvious spatial and temporal variation. The sediment incubation experiments (“sample” in supplementary Figure 1) at P01 indicated that the CH_4 concentration in the overlying waters increased linearly with incubation time (t) (March: $[CH_4] = 0.59\times t + 6.33$, $r^2 = 0.73$; October: $[CH_4] = 0.19\times t + 2.64$, $r^2 = 0.85$;

December: $[CH_4] = 0.23\times t + 4.37$, $r^2 = 0.95$), and the sediment-water CH_4 flux at P01 was 1.93 $\mu mol\cdot m^{-2}\cdot d^{-1}$ during March, 0.72 $\mu mol\cdot m^{-2}\cdot d^{-1}$ during October and 1.60 $\mu mol\cdot m^{-2}\cdot d^{-1}$ during December, respectively. Station C1 (near the Changjiang river mouth) had a sediment-water CH_4 flux of 2.94 $\mu mol\cdot m^{-2}\cdot d^{-1}$ during August, much higher than any other sites; this might be ascribed to the low oxygen concentration in the overlying water (3.25 $mg\cdot L^{-1}$ based on Winkler titration) and the rich organic carbon in the sediment (Lin et al., 2002; Kao et al., 2003).

Due to the limit of weather and lab resources, our sediment collection in August 2011 mainly covered the coastal areas. To avoid spatial bias induced by our sampling area, we added the sediment-water CH_4 fluxes obtained from a cruise in August 2013 (Figure 1, stations labelled by the black star) to provide data for the shelf and slope regions. As estimated, average sediment-water CH_4 flux from the ECS and YS was about 1.06 and 0.73 $\mu mol\cdot m^{-2}\cdot d^{-1}$ in 2011, respectively. Based on their surface areas (about 7.7×10^5 and 3.8×10^5 km^2), the annual CH_4 emission from sediments of the ECS and YS in 2011 was about 2.98×10^8 and 1.01×10^8 mol, respectively. This indicated that sediments were an important source of CH_4 in the bottom waters. However, the estimate of CH_4 released from the sediment had great uncertainties because of the scant sampling stations in each survey and the high spatial variation of sediment-water CH_4 flux.

3.6 Sea-air CH_4 fluxes in the YS and ECS

To eliminate the influence of large spatial difference, we divided the sampling region into four subareas, estimated the area using grid method and calculated the sea-air fluxes with N2000 and W2014 for each subarea. The CH_4 saturation and average area-weighed sea-air flux density were shown in Table 3. CH_4 saturation in the YS had an obvious seasonal variation, with that in autumn much higher than in spring. However, Yang et al. (2010) reported that average surface CH_4 saturation in the YS was highest (515.2% ± 231.5%) during August. Surface CH_4 saturations in the ECS also showed seasonal variation, with the maximum CH_4 saturation occurring in summer, followed by late spring, autumn, winter and early spring. These results were consistent with the results reported by Ye et al. (2015). Highest CH_4 saturation was observed at the Changjiang Estuary. We recorded the highest CH_4 saturation at station T05 (1007%) in March, station C0 (858%) in May, and station E01 (1558%) in August. In general, the surface waters of the YS and ECS were all oversaturated with atmospheric CH_4, except for some sporadic stations during spring. Thus, the YS and the ECS were net sources of atmospheric CH_4.

Sea-air CH_4 fluxes calculated using the N2000 equation were quite similar to those estimated from the W2014 equation, and they also showed seasonal and spatial variations in the wide ECS shelf, with the highest CH_4 flux occurring in the late spring and the lowest in early spring. In August, although the estuary only covered 25% of total observation area, it was responsible for about 46% of total CH_4 emission from ECS. It indicated that sea-air exchange of CH_4 in coastal areas was extremely intense, much greater than on the shelf area. Sea-air CH_4 flux density in the shelf water of the ECS was about 11.61 $\mu mol \cdot m^{-2} \cdot d^{-1}$ during summer, which was much higher than the previous research (merely 2.81–6.89 $\mu mol \cdot m^{-2} \cdot d^{-1}$) by Zhang et al. (2008a). According to N2000 and W2014 equation, the annual average area-weighed sea-air CH_4 flux density of the ECS and YS was about 9.75 $\mu mol \cdot m^{-2} \cdot d^{-1}$ during 2011. Based on the areas of the YS (~380000 km^2) and ECS (~770000 km^2), we estimated the total CH_4 emission from them as 4.09×10^9 mol (about 0.065 Tg) during 2011. Bange (1994) estimated the global oceanic CH_4 emission was 11–18 Tg $CH_4 \cdot year^{-1}$, so the YS and ECS accounted for about 0.45% of the global oceanic emission. This value was much higher than its corresponding area proportion of 0.32%, indicating that the YS and ECS are active areas for CH_4 production and emission.

4 Discussion

4.1 Factors influencing CH_4 distribution in the ECS and YS

The concentration, saturation, and sea-air and sediment-water fluxes of CH_4 in the ECS and YS all had obvious seasonal variations. Mean CH_4 saturation (R_{CH4}) had a linear correlation with mean water temperature (T) in the surface water (R_{CH4} =

13.91×T – 30.10, r^2 = 0.77; Supplementary Figure 2) and bottom water (R_{CH4} = 33.50×T – 225.03, r^2 = 0.76; Supplementary Figure 2) during different seasons. Average sediment-water fluxes of CH_4 showed a weak correlation with average T (F_{CH4}=0.06T+0.03, R^2=0.3), suggesting that CH_4 emission from the sediments increases with temperature. It was reported that CH_4 production rate increases with temperature in the range of 0-30°C (Liikanen et al., 2002; Glissmann et al., 2004). Besides, the high temperature may enhance the relative abundance and diversity of methanogenic communities (Høj et al., 2008; Metje and Frenzel, 2005). Yvon-Durocher et al. (2014) reported seasonal variations of CH_4 emissions from diverse ecosystems using meta-analysis, and showed that CH_4 emissions increased significantly with seasonal increases of temperature due to increase of CH_4 production from methanogens and anaerobic microbial communities. Our results were consistent with these previous studies, and supported the view that water temperature played an important role in regulating the seasonal variation and distribution of CH_4 in the ECS and YS.

The sediment incubation experiments and the depth profile of CH_4 in the ECS all indicated that sediment release was a significant source of CH_4 in bottom waters, especially at the shelf break area. Lin et al. (1992) found that organic carbon concentrations in bottom sediments increased across the shelf break, and were greatest in sediments at depths of 1000-1500 m in the ECS, suggesting that high CH_4 in bottom waters may come from high CH_4 production and subsequent release from the organic-rich sediments. Previous studies also showed that many submarine mud volcanoes and hydrothermal vents occur along the continental slope of the ECS (Zhao et al., 2006; Kawagucci et al., 2011). Methane-containing fluid was episodically vented, then transported to the water column. CH_4 in the hydrothermal fluid has been considered as a thermogenic origin and the CH_4 level may be 10^4-10^7 times higher than those in the ambient seawater (Kawagucci et al., 2011). When released from the vent, it forms buoyant plumes rapidly (Tsunogai et al., 2000). During the dilution, CH_4 can be oxidized quickly in the plume due to the microbial oxidation (De Angelis et al., 1993). The residual CH_4 spreads into the upper seawater. Hence, CH_4 release from sediments, mud volcanoes and hydrothermal fluids may also influence the CH_4 distribution in the bottom waters, especially at the continental slope.

CH_4 formation and consumption in the water column are also important factors that influence the distribution of CH_4 in the ECS and YS. Subsurface methane maxima were observed in this study, which have been considered to be a common phenomenon in the open sea (Reeburgh, 2007). Early studies demonstrated that advective transport of CH_4 or *in situ* CH_4 production by microbes in anoxic microenvironments led to excess CH_4 in the mixed layer (Scranton and Brewer, 1977; De Angelis and Lee, 1994; Karl and Tilbrook, 1994). More recent results suggest that under conditions with rich oxygen and specific nutrient limitation, a variety of methyl-rich organic phosphorus or sulfur compounds were all likely to be utilized by microorganisms and served as precursors of CH_4 production (Karl et al., 2008; Damm et al., 2008; Zindler et al., 2013; Florez-Leiva et al., 2013). The bottom water incubation experiments ("blank" in section 2.2 and in Supplementary Figure 1) at some stations (L1 in May, J1 in August, A10 and A02 in October and R07 in December) in this study indicated that CH_4 concentration increased linearly with incubation time. This suggested that *in situ* CH_4 production might be another source of the excess CH_4 in the bottom waters. Moreover, CH_4 production in the water column can be enhanced by hypoxia (Ye et al., 2015). Extremely high bottom CH_4 values (20-26 nM) were found near the Changjiang Estuary and outside Hangzhou Bay during August 2011, together with low oxygen level (2.00-4.00 mg/L) and high particulate organic carbon flux (3900-7300 mg $C\cdot m^{-2}\cdot d^{-1}$; Hung et al., 2013). Both high bottom water production and sediment release may contribute to this.

Riverine input plays an important role in regulating the distribution of CH_4 in the YS and ECS. CH_4 concentration in the river water of Changjiang was about 10-40 times higher than that of the ECS (Zhang et al., 2004; 2008), and the freshwater discharge from the Changjiang during summer was much greater than during winter (Table 4), therefore the widespread dispersal of Changjiang plume had a great impact on CH_4 distribution, especially in summer. Similar to the CDW, the Kuroshio and TWCW had different effects on the ECS during summer and winter. During summer, water input from the TWCW (2.39×10^6 $m^3·s^{-1}$) was much greater than that from the Kuroshio (0.89×10^6 $m^3·s^{-1}$) (Zhang et al., 2007), and the CH_4 level of the TWCW (6.11 mol·L^{-1}, Ye et al., 2015) was almost two-fold of that in the Kuroshio (2.91 mol·L^{-1}). Thus, the TWCW had a greater influence on CH_4 distribution in the ECS than the Kuroshio during summer, while they had comparable influence during winter due to similar water discharges and CH_4 concentrations. Thus, the mixing of different water masses and their seasonal variations directly impact CH_4 distribution in the ECS.

Submarine groundwater discharge (SGD) has been recognized as an important pathway for material transport to the marine environments (Burnett et al., 2006). It usually contains high levels of CH_4, and can serve as an important CH_4 source for the coastal ocean (Bugna et al., 1996; Corbett et al., 2000; Santos et al., 2009; Lecher et al., 2015). SGD is a mixture of fresh groundwater and recirculated seawater, and there is no CH_4 data available for either of them for the ECS. We collected some groundwater samples as fresh groundwater end-member along the coast of the ECS in December 2011 and July 2012. During December 2011, groundwater samples were collected at twenty-five sites along the Jiangsu and Zhejiang coastal region (120.857~121.896°E, 30.124~30.956°N). CH_4 concentrations varied significantly at these stations with a great range of 33~61602 nM and a median of 271 nM (Zhang et al., unpublished data). During July 2012, eight groundwater samples for CH_4 measurement were collected along the coast of the ECS (121.371~121.934°E, 30.733~31.976°N). CH_4 concentrations ranged between 138 and 3428 nM with a median of 758 nM. CH_4 concentrations in fresh groundwater end-member along the coast of the ECS were much higher than those in the seawater. Hence submarine ground water discharge might be an important CH_4 source for the East China Sea and could influence its CH_4 distribution.

4.2 Preliminary estimate of CH_4 budget in the ECS

In order to quantify the contributions of different sources and sinks to dissolved CH_4 in the ECS, CH_4 budget was estimated preliminary based on data presented here and collected from previous research. Zhang et al. (2007) re-estimated the nutrient budget of the ECS using a box model during summer and winter. According to mass conservation, the water and salinity balance of the ECS can be expressed as:

$$\sum_{i=1}^{n} WFi + \Delta Q = 0 \quad (3)$$

$$\sum_{i=1}^{n} WFi \times Ci + \Delta Mi = 0 \quad (4)$$

where *WFi* represents the water flux of inputs (+) and outflows (-) over the shelf; ΔQ is the water mass distinction caused by sea level change in the ECS; *Ci* is the salinity or value of a certain element for a known water mass; and ΔMi is the increase or decrease of the given element during exchange at the sediment-water and sea-air interface. The inflow to the ECS Shelf includes water from the Taiwan Strait (TWCW), riverine input from the land-mass (of which the Changjiang accounts for about 90–95% or more), and incursion of the Kuroshio from north of Taiwan and over the broad shelf mainly composed of KSW (~25%) and KSSW (~75%) (Zhang et al., 2007). The exchange between the ECS and the YS is taken into account as well. The outflow refers to currents through the Tsushima/Korea Strait (Zhang et al., 2007).

As with the shelf water budget in the ECS (Zhang et al., 2007), we estimated the budget of dissolved CH_4 for summer and winter. The Kuroshio and TWCW were hardly observed during our summer cruise because of the limited investigation region, so the corresponding data were from the literature (Ye et al., 2015) and unpublished data for the ECS that was collected in July 2013. Data for riverine CH_4 were from our on-going monitoring project at station Xuliujing (121°2´ E, 31°46´ N), which is the most downstream main channel station at the Changjiang. Considering that the sea-air fluxes values from W2014 and N2000 relationships were quite similar, we took those estimated by W2014 for budget calculation. Submarine groundwater discharge (SGD) data for the ECS is rather limited. Gu et al. (2012) estimated the SGD in the Changjiang effluent plume to be about (0.2-1.0) × 10^9 m^3d^{-1} during summer and no

SGD data is available for the whole ECS in literature yet. Hence it is difficult to estimate the CH_4 input to ECS via SGD quantitatively. Fortunately, Prof. Jinzhou Du from East China Normal University provided us their update and unpublished SGD data obtained using Ra isotopes as tracers for the ECS (including submarine fresh water discharge and recirculated saline groundwater discharge), which is 0.68×10^8 m^3 d^{-1} and 0.46×10^9 m^3 d^{-1} in dry and wet season, respectively (Du et al., unpublished data, personal communication). It is hard to determine CH_4 concentrations in the recirculated seawater, so we assume that CH_4 concentrations in the fresh groundwater and recirculated saline groundwater are the same. Median CH_4 concentration was chosen for calculation since it is less susceptible to abnormally high CH_4 concentrations observed in the groundwater. Hence, CH_4 fluxes via submarine groundwater discharge were estimated by multiplying the median CH_4 concentration by the SGD, which yielded a flux of 0.21 mol/s and 4.01 mol/s for winter and summer, respectively. SGD is a mixture of fresh groundwater and recirculated seawater, among which the latter could account for 90% of the discharge or more (Burnett et al., 2006), but considering CH_4 concentration in the porewaters (~0.45 μM, Zhang et al., unpublished data) of the ECS usually is much lower than those in fresh groundwater, the above estimation of CH_4 flux via submarine groundwater discharge may be overestimated to some extent.

Table 4 lists the discharges of various water masses and their CH_4 concentrations, and Figure 8 shows a preliminary estimate of the CH_4 budget in the ECS. We ignored the effects of evaporation and precipitation because of unavailable data and the low water fluxes of these processes. During summer, the TWCW transported 14.60 $mol\cdot s^{-1}$ of CH_4 to the ECS via Taiwan Strait, the Kuroshio transported 2.97 $mol\cdot s^{-1}$ of CH_4, the CH_4 input from CDW is 3.45 $mol\cdot s^{-1}$, and sediment released 14.70 $mol\cdot s^{-1}$ of CH_4. Groundwater might contribute 4.01 $mol\cdot s^{-1}$ CH_4 to the ECS, which is comparable to the input via river runoff. However, CH_4 emission at the sea-air interface reached 138.40 $mol\cdot s^{-1}$ and CH_4 export from the ECS was 18.12 $mol\cdot s^{-1}$. Consequently, to maintain a balance of the CH_4 in the ECS, the rate of *in situ* net CH_4 formation (i.e.

CH_4 production-CH_4 oxidation) should be 116.73 mol·s^{-1}, which contributed more than 70% of the CH_4 sources in summer.

During winter, the Kuroshio imported 5.28 mol·s^{-1} of CH_4 into the ECS (1.8-fold more than in summer), and the TWCW imported 5.20 mol·s^{-1} of CH_4 (1/3 of that in summer). Although the winter discharge of the Changjiang was almost equal with the water inflow YS, CH_4 input by Changjiang (2.11 mol·s^{-1}) was significantly higher than that from the YS (0.06 mol·s^{-1}). CH_4 emission from sediments was 8.38 mol·s^{-1} and CH_4 input from groundwater was about 0.21mol/s during winter (only 5% of that in summer). CH_4 release from the ECS into the atmosphere was about 81.28 mol·s^{-1} and the CH_4 export out of the ECS was 13.14 mol·s^{-1}. Thus, the net CH_4 production rate of seawater during winter was inferred to be 73.18 mol·s^{-1} to balance the CH_4 loss by sea-air exchange and outflow.

However, the above results were merely a rough estimate with large uncertainties. Firstly, there were potential errors involved in the measurements and calculations of sea-air fluxes. Secondly, the estimation of CH_4 input via SGD was quite crude due to the limited available data about SGD and groundwater CH_4. Thirdly, we performed sediment incubations only at several stations during each survey, and the results were far from representative of sediment emission from the whole ECS due to large spatial and seasonal variations. Finally, some CH_4 sources and sinks were neglected in this estimation. For example, aerobic CH_4 oxidation has been shown to be a substantial sink of CH_4, however, no estimates of methane oxidation extents and rates were made in the water column here. Seepage of thermogenic methane from the sediments was also ignored due to lack of data. Hence the role of net in situ microbial production might be exaggerated by estimating it as the difference between sources and sinks. Although our method of estimation was not perfect, we demonstrated a variety of CH_4 sources and sinks for the ECS and roughly estimated their relative contribution. It suggests that in situ production in the water column and sediment emissions are major CH_4 sources in the marginal shelf seas, while sea-to-air release was the major external sink of CH_4 in the ECS. Groundwater might be an important source of CH_4 in the

ECS, especially in wet seasons. Hence more research work on CH_4 production and consumption as well as CH_4 in groundwater discharge is needed to further understand the CH_4 budget in the ECS.

5 Conclusions

CH_4 distribution and emission in the ECS and YS had obvious spatial and seasonal variations, and were also influenced by various factors, including mixing of different water masses, water temperature, freshwater input, sediment release, hydrothermal seepage and oxygen levels in the water column. We estimated the CH_4 budget of the ECS using a box model, and the results indicated that in situ seawater production and sediment release might be the major CH_4 source, while sea-air exchange was the major external sink of CH_4 in the ECS. Groundwater might be an important source of CH_4 in the ECS, especially in wet seasons. The ECS and the YS together was estimated to release about 4.09×10^9 mol of CH_4 per year into the atmosphere, which accounts for about 0.45% of the global oceanic emission and was much higher than its corresponding area proportion of 0.32%. Hence the YS and ECS were active areas for CH_4 production and emission.

Author contributions

M.-S. Sun collected and analyzed water samples in October and December 2011. G.-L. Zhang designed the sampling strategy. M.-S. Sun and G.-L. Zhang prepared the manuscript. X.-P. Cao collected and analyzed water samples in March, May, and August 2011. X.-Y. Mao provided hydrological data for March, October and December of 2011. J. Li provided hydrological data for May and August of 2011. W.-W. Ye provided some data for calculation of the methane budget of the East China Sea.

Acknowledgements

The authors wish to thank the crews of the R/V “Dong Fang Hong 2”, the R/V

“BeiDou” and the R/V “Experiment 3” and colleagues from the Laboratory of Marine Biogeochemistry, Ocean University of China for assistance in collection of field samples. Prof. Jinzhou Du from East China Normal University was acknowledged to provide us SGD data. Besides, we are grateful to Prof. Hermann W. Bange for his suggestions about the revision of this manuscript. This study was funded by the Ministry of Science and Technology of China through Grant no. 2011CB409802, 2010CB428904 and 2011CB409803 supported by the National Science Foundation of China through Grant nos. 41221004, and by the 111 Project (B13030). This is MCTL Contribution no. 76. M.-S. Sun is especially grateful for the scholarship provided by the China Scholarship Council during her study in Germany.

References

Aller, R. C., Mackin, J. E., Ullman, W. J., Chen-Hou, W., Shing-Min, T., Jian-Cai, J., Yong-nian, S. and Jia-Zhen, H.: Early chemical diagenesis, sediment-water solute exchange, and storage of reactive organic matter near the mouth of the Changjiang, East China Sea, Cont. Shelf Res., 4(1), 227-251, doi: 10.1016/0278-4343(85)90031-7, 1985.

Bange, H. W., Bartell, U. H., Rapsomanikis, S., and Andreae, M. O.: Methane in the Baltic and North Seas and a reassessment of the marine emissions of methane, Global Biogeochem. Cy., 8(4), 465-480, doi: 10.1029/94GB02181, 1994.

Bange, H. W.: Air-sea exchange of nitrous oxide and methane in the Arabian Sea: A simple model of the seasonal variability, Indian J. Mar. Sci., 33(1), 77-83, 2004.

Bange, H. W., Bell, T. G., Cornejo, M., Freing, A., Uher, G., Upstill-Goddard, R. C., and Zhang, G. L.: MEMENTO: a proposal to develop a database of marine nitrous oxide and methane measurements, Environ. Chem., 6(3), 195-197, 2009.

Barnes, J., and Owens, N. J. P.: Denitrification and nitrous oxide concentrations in the Humber estuary, UK, and adjacent coastal zones, Mar. Pollut. Bull., 37(3), 247-260, doi:10.1016/S0025-326X(99)00079-X, 1999.

Bryan, J. R., Rlley, J. P., and Williams, P. L.: A Winkler procedure for making precise measurements of oxygen concentration for productivity and related studies, J. Exp. Mar. Biol. Ecol., 21(3), 191-197, doi: 10.1016/0022-0981(76)90114-3, 1976.

Bugna, G. C., Chanton, J. P., Cable, J. E., Burnett, W. C., and Cable, P. H.: The importance of groundwater discharge to the methane budgets of nearshore and continental shelf waters of the northeastern Gulf of Mexico, Geochim. Cosmochim. Ac., 60(23), 4735-4746, doi: 10.1016/S0016-7037(96)00290-6, 1996.

Burnett, W. C., Aggarwal, P. K., Aureli, A., Bokuniewicz, H., Cable, J. E., Charette, M.

A., Kontar, E., Krupa, S., Kulkarni, K. M., Loveless, A., Moore, W. S., Oberdorfer, J. A., Oliveira, J., Ozyurt, N., Povinec, P., Priviyera, A. M. G., Rajar, R., Ramessur, R. T., Scholten, J., Stieglitz, T., Taniguchi, M., and Turner, J. V.: Quantifying submarine groundwater discharge in the coastal zone via multiple methods, Sci. total Environ., 367(2), 498-543, 2006.

Changjiang Sediment Bulletin 2011, edited by Changjiang Water Resources Committee, P. R. C. Minister of Water Resources, Changjiang Press, Wuhan, China, 43 pp., 2011.

Cockenpot, S., Claude, C., Radakovitch, O.: Estimation of air-water gas exchange coefficient in a shallow lagoon based on ^{222}Rn mass balance, J. Environ. Radioactiv., 143 (2015), 58-69, doi:10.1016/j.jenvrad.2015.02.007, 2015.

Corbett, D. R., Dillon, K., Burnett, W., and Chanton, J.: Estimating the groundwater contribution into Florida Bay via natural tracers, ^{222}Rn and CH_4, Limnol. Oceanogr., 45(7), 1546-1557, doi: 10.4319/lo.2000.45.7.1546, 2000.

Crutzen, P. J., and Zimmermann, P. H.: The changing photochemistry of the troposphere, Tellus B, 43(4), 136-151, 1991.

Damm, E., Kiene, R. P., Schwarz, J., Falck, E., and Dieckmann, G.: Methane cycling in Arctic shelf water and its relationship with phytoplankton biomass and DMSP, Mar. Chem., 109(1), 45-59, doi:10.1016/j.marchem.2007.12.003, 2008.

De Angelis, M. A., M. D. Lilley, and J. A. Baross.: Methane oxidation in deep-sea hydrothermal plumes of the Endeavour Segment of the Juan de Fuca Ridge, Deep-Sea Res. Pt I, 40 (6), 1169-1186, doi:10.1016/0967-0637(93)90132-M, 1993.

De Angelis, M. A. and Lee, C.: Methane production during zooplankton grazing on marine phytoplankton, Limnol. Oceanogr., 39(6), 1298-1308, 1994.

ESRL's Global Monitoring Division: http://www.esrl.noaa.gov/gmd, last access: 6th April 2015.

Florez-Leiva, L., Damm, E., and Farías, L.: Methane production induced by dimethylsulfide in surface water of an upwelling ecosystem, Prog. Oceanogr., 112, 38-48, doi:10.1016/j.pocean.2013.03.005, 2013.

Forster, G., Upstill-Goddard, R. C., Gist, N., Robinson, C., Uher, G., and Woodward, E. M. S.: Nitrous oxide and methane in the Atlantic Ocean between 50°N and 52°S: Latitudinal distribution and sea-to-air flux, Deep-Sea Res. Pt II, 56(15), 964-976, doi:10.1016/j.dsr2.2008.12.002, 2009.

Gao, L., Li, D., Zhang, Y.: Nutrients and particulate organic matter discharged by the Changjiang (Yangtze River): Seasonal variations and temporal trends. J. Geophys. Res.-Biogeo. (2005–2012), 117(G4), doi: 10.1029/2012JG001952, 2012.

Glissman, K., Chin, K. J., Casper, P., and Conrad, R.: Methanogenic pathway and archaeal community structure in the sediment of eutrophic Lake Dagow: effect of temperature, Microb. Ecol., 48(3), 389-399, doi: 10.1007/s00248-003-2027-2, 2004.

Gu, H., Moore, W. S., Zhang, L., Du, J., and Zhang, J.: Using radium isotopes to estimate the residence time and the contribution of submarine groundwater discharge (SGD) in the Changjiang effluent plume, East China Sea, Cont. Shelf Res., 35, 95-107, doi: 10.1016/j.csr.2012.01.002, 2012.

Høj, L., Olsen, R. A. and Torsvik, V. L.: Effects of temperature on the diversity and community structure of known methanogenic groups and other archaea in high Arctic peat, The ISME journal, 2(1), 37-48, doi:10.1038/ismej.2007.84, 2008.

Hung, C. C., Tseng, C. W., Gong, G. C., Chen, K. S., Chen, M. H., and Hsu, S. C.: Fluxes of particulate organic carbon in the East China Sea in summer, Biogeosciences, 10(10), 6469-6484, doi:10.5194/bg-10-6469-2013, 2013.

IPCC, 2013: climate change 2013: the physical science basis. Contribution of working group I to the fifth assessment report of the intergovernmental panel on climate change, edited by: Stocker, T. F., Qin, D., Plattner, G. K., Tignor, M., Allen, S. K., Boschung, J., Nauels A. Xia Y. Bex V. and Midgley, P. M., Cambridge University Press, Cambridge, United Kingdom and New York, NY, USA, 1535 pp., 2013.

Kao, S. J., Lin, F. J., and Liu, K. K.: Organic carbon and nitrogen contents and their isotopic compositions in surficial sediments from the East China Sea shelf and the southern Okinawa Trough, Deep-Sea Res. Pt II, 50(6), 1203-1217, doi:10.1016/S0967-0645(03)00018-3, 2003.

Karl D. M. and Tilbrook B. D.: Production and transport of methane in oceanic particulate organic matters, Natue, 368, 732-734, 1994.

Karl, D. M., Beversdorf, L., Björkman, K. M., Church, M. J., Martinez, A., and Delong, E. F.: Aerobic production of methane in the sea, Nat. Geosci., 1(7), 473-478, doi:10.1038/ngeo234, 2008.

Kawagucci, S., Chiba, H., Ishibashi, J. I., Yamanaka, T., Toki, T., Muramatsu, Y., Ueno, Y., Makabe, A., Inoue, K., Yoshida, N., Nakagawa, S., Nunoura, T., Takai, K., Takahata, N., Sano, Y., Narita, T., Teranishi, G., Obata, H. and Gamo, T.: Hydrothermal fluid geochemistry at the Iheya North field in the mid-Okinawa Trough: Implication for origin of methane in subseafloor fluid circulation systems, Geochem. J., 45(2), 109-124, 2011.

Kock, A., Gebhardt, S., and Bange, H. W.: Methane emissions from the upwelling area off Mauritania (NW Africa), Biogeosciences, 5, 1119-1125, doi: 10.5194/bg-5-1119-2008, 2008.

Lecher, A. L., Kessler, J., Sparrow, K., Garcia-Tigreros Kodovska, F., Dimova, N., Murray, J., Tulaczyk, S., and Paytan, A.: Methane transport through submarine groundwater discharge to the North Pacific and Arctic Ocean at two Alaskan sites. Limnol. Oceanogr., doi: 10.1002/lno.10118, 2015.

Liikanen, A. N. U., Murtoniemi, T., Tanskanen, H., Väisänen, T., and Martikainen, P. J.: Effects of temperature and oxygenavailability on greenhouse gas and nutrient dynamics in sediment of a eutrophic mid-boreal lake, Biogeochemistry, 59(3), 269-286, 10.1023/A:1016015526712, 2002.

Li, F. Q., Su, Y. S.: Analysis of Sea Water Masses, Qingdao Ocean University Press, Qingdao, China, pp. 379, 2000. (in Chinese)

Lin, S., Liu, K.K., Chen, M.P., Chang, F.Y.: Distribution of organic carbon in the KEEP area continental margin sediments, Terr. Atmos. Ocean. Sci., 3(3), 365-378, 1992.

Lin, S., Hsieh, I. J., Huang, K. M., and Wang, C. H.: Influence of the Yangtze River and grain size on the spatial variations of heavy metals and organic carbon in the East China Sea continental shelf sediments, Chem. Geol., 182(2), 377-394, doi:10.1016/S0009-2541(01)00331-X, 2002.

Metje, M. and Frenzel, P.: Effect of temperature on anaerobic ethanol oxidation and methanogenesis in acidic peat from a northern wetland, Appl. Environ. Microb., 71(12), 8191-8200, doi: 10.1128/AEM.71.12.8191-8200.2005, 2005.

Nightingale, P. D., Malin, G., Law, C. S., Watson, A. J., Liss, P. S., Liddicoat, M. I., Boutin, J. and Upstill-Goddard, R. C.: In situ evaluation of air-sea gas exchange parameterizations using novel conservative and volatile tracers, Global Biogeochem. Cy., 14(1), 373-387, doi: 10.1029/1999GB900091, 2000.

Qi, J., Yin, B., Zhang, Q., Yang, D. and Xu, Z.: Analysis of seasonal variation of water masses in East China Sea, Chin. J. Oceanol. Limn., 32(4), 958-971, doi: 10.1007/s00343-014-3269-1, 2014.

Quay, P., Stutsman, J., Wilbur, D., Snover, A., Dlugokencky, E. and Brown, T.: The isotopic composition of atmospheric methane, Global Biogeochem. Cy., 13(2), 445-461, doi: 10.1029/1998GB900006, 1999.

Reeburgh, W. S.: Oceanic methane biogeochemistry, Chem. Rev., 107(2), 486-513, doi: 10.1021/cr050362v, 2007.

Rehder, G., and Suess, E.: Methane and pCO_2 in the Kuroshio and the South China Sea during maximum summer surface temperatures. Mar. Chem., 75(1), 89-108, doi:10.1016/S0304-4203(01)00026-3, 2001.

Santos, I. R., Dimova, N., Peterson, R. N., Mwashote, B., Chanton, J., and Burnett, W. C.: Extended time series measurements of submarine groundwater discharge tracers (^{222}Rn and CH_4) at a coastal site in Florida. Mar. Chem., 113(1), 137-147, doi: 10.1016/j.marchem.2009.01.009, 2009.

Scranton, M. I. and Brewer, P. G.: Occurrence of methane in the near-surface waters of the western subtropical North-Atlantic, Deep-Sea Res., 24(2), 127-138, doi: 10.1016/0146-6291(77)90548-3, 1977.

Shakhova, N., Semiletov, I., Salyuk, A., Yusupov, V., Kosmach, D. and Gustafsson, Ö.: Extensive methane venting to the atmosphere from sediments of the East Siberian Arctic Shelf, Science, 327(5970), 1246-1250, doi: 10.1126/science.1182221, 2010.

Shen, Z.: A new method for the estimation of fine-sediment resuspension ratios in estuaries—taking the turbidity maximum zone of the Changjiang (Yangtze) estuary as an example, Chin. J. Oceanol. Limn., 30(5), 791-795, doi: 10.1007/s00343-012-2004-z, 2012.

Song, G., Liu, S., Zhu, Z., Zhai, W., Zhu, C., and Zhang, J: Sediment oxygen consumption and benthic organic carbon mineralization on the continental shelves of the East China Sea and the Yellow Sea, Deep-Sea Res. Pt II, in press, doi: 10.1016/j.dsr2.2015.04.012, 2015.

Su, J.: Circulation dynamics of the China Seas north of 18 °N, in: The Sea, vol. 11, edited by: Robinson, A. R. and Brink, K. H., John Wiley & Sons, New York, 483–505, 1998.

Tsunogai, U., Yoshida, N., Ishibashi, J. and Gamo, T..: Carbon isotopic distribution of methane in deep-sea hydrothermal plume, Myojin Knoll Caldera, Izu-Bonin arc: implications for microbial methane oxidation in the oceans and applications to heat flux estimation, Geochim. Cosmochim. Ac., 64 (14): 2439-2452, doi:10.1016/S0016-7037(00)00374-4, 2000.

Tsurushima, N., Watanabe, S. and Tsunogai, S., Methane in the East China Sea water,

J. Oceanogr., 52(2), 221-233, doi: 10.1007/BF02235671, 1996.

Wang, H., Yang, Z., Wang, Y., Saito, Y. and Liu, J. P.: Reconstruction of sediment flux from the Changjiang (Yangtze River) to the sea since the 1860s, J. Hydrol., 349(3), 318-332, doi:10.1016/j.jhydrol.2007.11.005, 2008.

Wanninkhof R.: Relationship between wind speed and gas exchange over the ocean, J. Geophys. Res.-Oceans (1978–2012), 97(C5), 7373-7382, 1992.

Wanninkhof R.: Relationship between wind speed and gas exchange over the ocean revisited, Limnol. Oceanogr.-Meth., 12(6), 351–362, doi: 10.4319/lom.2014.12.351, 2014.

Wiesenburg, D. A. and Guinasso Jr, N. L.: Equilibrium solubilities of methane, carbon monoxide, and hydrogen in water and sea water, J. Chem. Eng. Data, 24(4), 356-360, doi: 10.1021/je60083a006, 1979.

Yvon-Durocher, G., Allen, A. P., Bastviken, D., Conrad, R., Gudasz, C., St-Pierre, A. Thanh-Duc, N. and Del Giorgio, P. A.: Methane fluxes show consistent temperature dependence across microbial to ecosystem scales, Nature, 507(7493), 488-491, doi: 10.1038/nature13164, 2014.

Yang, J., Zhang, G. L., Zheng, L. X., Zhang, F. and Zhao, J.: Seasonal variation of fluxes and distributions of dissolved methane in the North Yellow Sea, Cont. Shelf Res., 30(2), 187-192, doi: 10.1016/j.csr.2009.10.016, 2010.

Ye, W., Zhang, G., Zhu, Z., Huang, D., Han, Y., Wang, L. and Sun, M.: Methane Distribution and Sea-to-Air Flux in the East China Sea During the Summer of 2013: Impact of Hypoxia, Deep-Sea Res. Pt II, in press, 2015.

Yuan, D., Zhu, J., Li, C., and Hu, D.: Cross-shelf circulation in the Yellow and East China Seas indicated by MODIS satellite observations. J. Marine Syst., 70(1), 134-149, doi:10.1016/j.jmarsys.2007.04.002, 2008.

Zhang, G. L., Zhang, J., Kang, Y. B. and Liu, S. M.: Distributions and fluxes of methane in the East China Sea and the Yellow Sea in spring, J. Geophys.

Res.-Oceans (1978–2012), 109(C07011), doi:10.1029/2004JC002268, 2004.

Zhang, G., Zhang, J., Ren, J., Li, J. and Liu, S.: Distributions and sea-to-air fluxes of methane and nitrous oxide in the North East China Sea in summer, Mar. Chem., 110(1), 42-55, doi: 10.1016/j.marchem.2008.02.005, 2008a.

Zhang, G., Zhang, J., Liu, S., Ren, J., Xu, J. and Zhang, F.: Methane in the Changjiang (Yangtze River) Estuary and its adjacent marine area: riverine input, sediment release and atmospheric fluxes, Biogeochemistry, 91(1), 71-84, doi: 10.1007/s10533-008-9259-7, 2008b.

Zhang, J.: Nutrient elements in large Chinese estuaries, Cont. Shelf Res., 16(8), 1023-1045, doi:10.1016/0278-4343(95)00055-0, 1996.

Zhang, J., Liu, S. M., Ren, J. L., Wu, Y. and Zhang, G. L.: Nutrient gradients from the eutrophic Changjiang (Yangtze River) Estuary to the oligotrophic Kuroshio waters and re-evaluation of budgets for the East China Sea Shelf, Prog. Oceanogr., 74(4), 449-478, 2007.

Zhao, H.Q., Wu, S.G., Xu, N., Wang, X.J., Zhang, G.X.: The Elementary Research of Gas Hydrate Associated with Mud Diapir Structure in the East China Sea, Geoscience 20 (1), 115-122, 2006. (in Chinese with English Abstract).

Zindler, C., Bracher, A., Marandino, C. A., Taylor, B., Torrecilla, E., Kock, A. and Bange, H. W.: Sulphur compounds, methane, and phytoplankton: interactions along a north-south transit in the western Pacific Ocean, Biogeosciences, 10(5), 3297-3311, doi: 10.5194/bg-10-3297-2013, 2013

Table 1. Characteristics of the five cruises in the East China Sea and the Yellow Sea.

Survey period	Research vessel	CTD	Station no.
13 Mar. - 10 Apr., 2011	Dong Fang Hong 2	Sea-Bird 911 plus	42
11 May - 7 June, 2011	Experiment 3	Sea-Bird 911 plus	54
10-30 August, 2011	Bei Dou	Sea-Bird 917	38
16 Oct. - 8 Nov., 2011	Dong Fang Hong 2	Sea-Bird 911 plus	55
20 Dec. 2011-7 Jan., 2012	Dong Fang Hong 2	Sea-Bird 911 plus	46

Table 2. Temperature, salinity, and CH_4 concentrations in surface and bottom waters of the Yellow Sea and East China Sea during five cruises in 2011. Numbers indicate ranges and average ± SD (SD gives the average difference between the average value and the individual values).

Season	Depth	Temperature (°C)	Salinity (psu)	CH_4 (nmol·L^{-1})
March	surface	4.32~19.03 (10.68 ± 3.06)	29.79~34.60 (33.16 ± 1.08)	2.39~29.67 (4.47 ± 4.09)
	bottom	5.48~16.13 (10.06 ± 2.40)	32.00~34.49 (33.26 ± 0.75)	2.63~30.63 (5.10 ± 4.97)
May	surface	16.40~26.17 (21.57 ± 3.00)	30.45~34.59 (33.14 ± 1.40)	1.88~26.39 (6.04 ± 5.58)
	bottom	4.00~23.92 (15.78 ± 4.62)	24.21~34.90 (33.07 ± 1.99)	1.31~30.36 (6.41 ± 5.11)
August	surface	21.93~28.25 (25.91 ± 1.45)	22.57~33.99 (30.22 ± 2.72)	3.71~33.62 (8.21 ± 6.02)
	bottom	9.01~24.99 (20.75 ± 2.98)	28.69~34.47 (33.02 ± 1.62)	6.20~26.22 (11.88 ± 4.59)
October	surface	17.89~26.18 (21.91 ± 2.26)	28.06~34.46 (32.84 ± 1.47)	2.44~13.52 (5.03 ± 1.68)
	bottom	4.12~24.19 (17.38 ± 5.43)	30.87~34.67 (33.41 ± 1.23)	2.50~15.24 (7.51 ± 2.93)
December	surface	7.94~23.46 (15.23 ± 4.28)	29.87~34.70 (33.33 ± 1.22)	3.01~6.03 (4.07 ± 0.63)
	bottom	7.84~23.45 (14.83 ± 4.08)	30.91~34.73 (33.48 ± 1.07)	3.03~10.20 (4.53 ± 1.33)

Table 3. Surface CH_4 saturation, sea-air CH_4 fluxes and the average area-weighed flux density in the Yellow Sea and East China Sea.

Region	Months	Area ratio	$R(CH_4)$/%	U_{10} /$m\cdot s^{-1}$	F(W2014) ($\mu mol\cdot m^{-2}\cdot d^{-1}$)	F(N2000) ($\mu mol\cdot m^{-2}\cdot d^{-1}$)	average area-weighed flux density ($\mu mol\cdot m^{-2}\cdot d^{-1}$)
YS	Mar.	25%	94-148 (117)	2.2-12.1 (8.3)	-0.56-9.59 (2.31)	-0.55-9.09 (2.23)	0.57
	May	12.7%	94-161 (123)	6.4-10.3 (8.3)	-0.37-3.49 (2.05)	-3.8-3.64 (2.05)	0.26
	Aug.	---	---	---	---	---	---
	Oct.	41.2%	101-376 (218)	1.6-9.9 (5.1)	0.04-30.47 (6.42)	0.04-29.59 (6.59)	2.68
	Dec.	42.9%	105-238 (146)	2.9-13.6 (7.2)	0.31-16.58 (3.87)	0.39-15.52 (3.86)	1.62
Estuary	Mar.	0.1%	(1007)	(0.2)	(0.05)	(0.33)	1.9×10^{-4}
	May	3.1%	161-858 (490)	1.3-11.3 (5.8)	0.15-50.49 (26.54)	0.27-48.23 (27.00)	0.83
	Aug.	26.1%	172-1558 (578)	1.9-8.9 (5.7)	2.25-118.23 (27.22)	3.06-120.19 (28.34)	7.25
	Oct.	2.2%	(558)	(8.7)	(51.27)	(50.69)	0.11
	Dec.	---	---	---	---	---	---
ECS shelf	Mar.	75%	91-340 (139)	0.3-13.5 (7.9)	-1.85-52.57 (4.67)	-1.75-49.61 (4.52)	3.45
	May	76.3%	87-1049 (252)	1.2-23.6 (9.0)	-4.30-138.96 (16.36)	-3.99-129.83 (15.79)	12.27
	Aug.	73.9%	195-528 (287)	3.3-8.4 (6.2)	1.66-24.99 (11.40)	2.00-26.09 (11.82)	8.58
	Oct.	52.9%	128-317 (215)	0.8-11.9 (7.3)	0.72-27.51 (10.50)	0.85-26.26 (10.42)	5.53
	Dec.	54.8%	128-213 (163)	3.7-14.1 (8.9)	1.26-23.49 (8.42)	1.47-22.15 (8.15)	4.54
ECS slope	Mar.	---	---	---	---	---	---
	May	7.9%	93-157 (128)	4.5-15.2 (9.7)	-0.97-17.47 (4.81)	-0.94-16.19 (4.55)	0.37
	Aug.	---	---	---	---	---	---
	Oct.	3.7%	186-211 (199)	8.4-10.1 (9.2)	11.44-12.84 (12.14)	11.37-12.44 (11.90)	0.44
	Dec.	2.3%	(232)	(11.7)	(25.84)	(24.59)	0.58

Table 4. Data used for calculation of the CH_4 budget in the East China Sea.

Parameter	Summer	Winter
Water exchange between ECS and YS (Sv)	-0.009[a]	0.013[a]
Evaporation (Sv)	-0.0068[a]	-0.010[a]
Rainfall (Sv)	0.031[a]	0.0062[a]
Terrestrial input (Sv)	0.0393[a]	0.0122[a]
Taiwan Strait water (Sv)	2.39[a]	1.22[a]
Kuroshio water (Sv)	0.89[a]	1.81[a]
Outflow of ECS (Sv)	-3.33[a]	-3.05[a]
Groundwater discharge ($m^3 \cdot s^{-1}$)	5300	790
Avg. CH_4 concentration in Changjiang (nM)	87.90[b]	173.26[b]
Avg. CH_4 concentration in TWCW (nM)	6.11[c]	4.26
Avg. CH_4 concentration in Kuroshio (nM)	3.34[c]	2.91
Avg. CH_4 concentration in YS (nM)	6.56[d]	4.33
Avg. CH_4 concentration in shelf of ECS (nM)	5.44[c]	4.31
Avg. sea-air CH_4 flux ($\mu mol \cdot m^{-2} \cdot d^{-1}$)	15.53	9.12
Avg. sediment-water CH_4 flux ($\mu mol \cdot m^{-2} \cdot d^{-1}$)	1.65	0.94
Median groundwater CH_4 concentration (nM)	758	271

Note: Positive values represent water import from an external source and negative values represent water export from the ECS. 1 Sv =10^6 $m^3 \cdot s^{-1}$; a. data from Zhang et al. (2007); b. unpublished data from an on-going monitoring project at Xuliujing station in the lower Changjiang; c. data from Ye et al. (2015); d. unpublished data from observations in July 2013.

Figure captions:

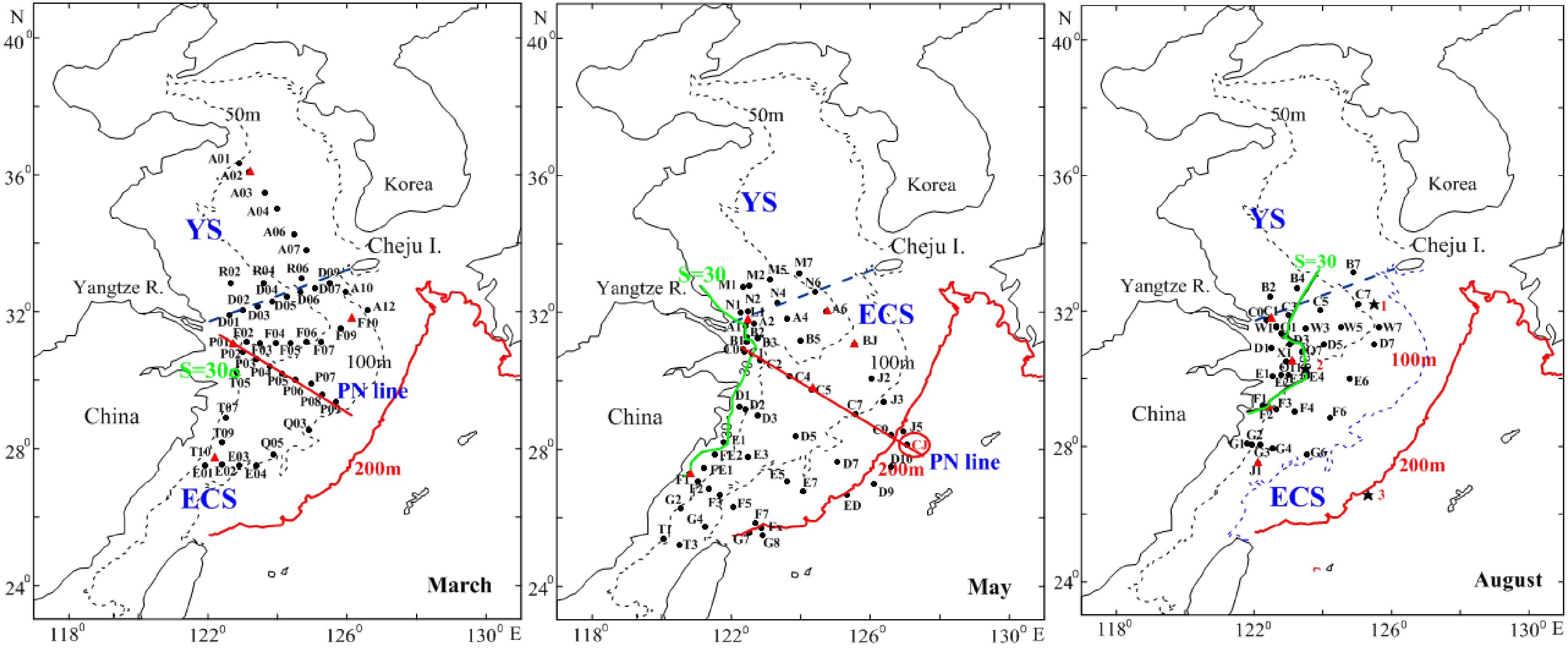

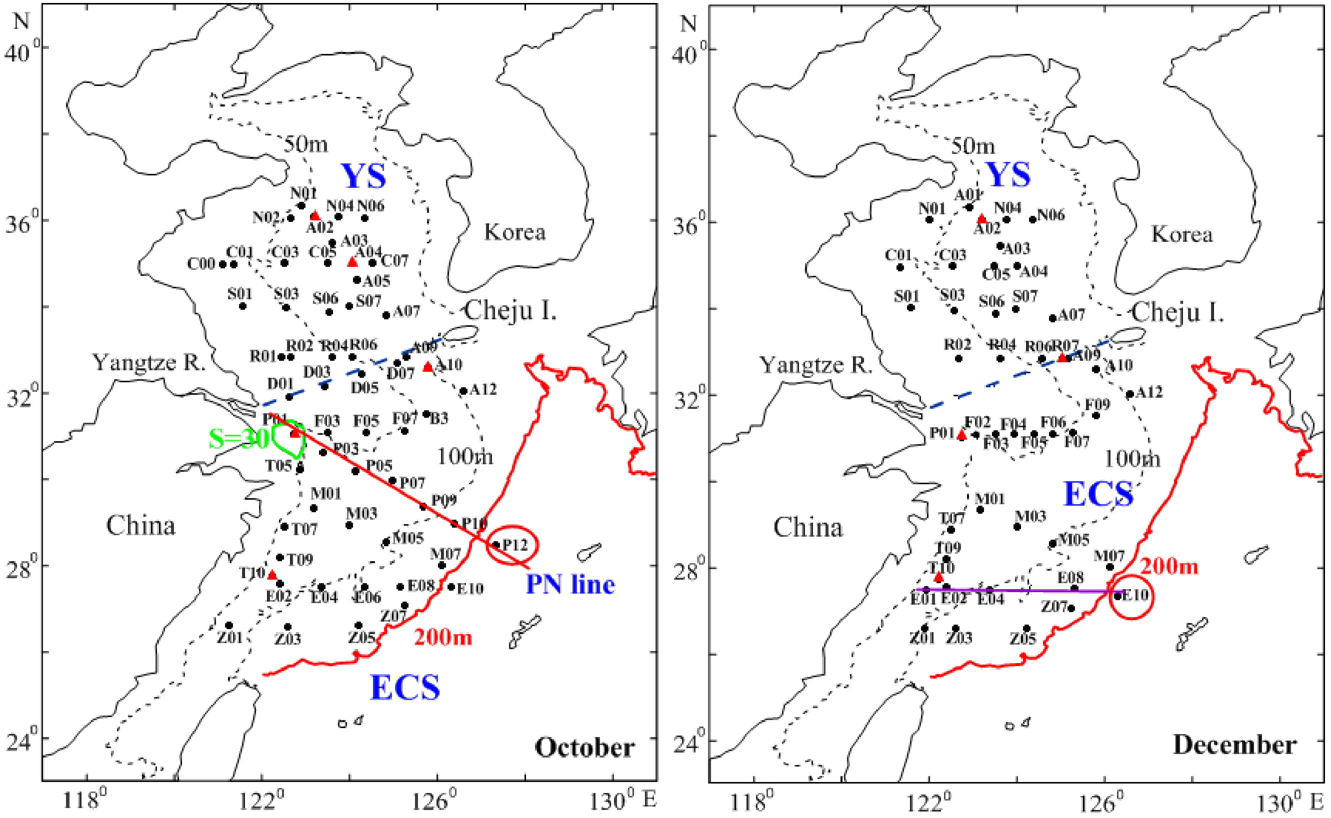

Fig. 1. Sampling locations in the East China Sea and the Yellow Sea during the five cruises in 2011. Black solid dots: seawater sampling locations; red solid triangles: sediment sampling locations; red solid line: PN line; blue dashed line: boundary between the East China Sea and the Yellow Sea; purple solid line: section E; red solid circle: the station depth more than 1000 m; red curve: the depth of 200 m line; the red curve: the salinity of 30 line; black star in August: sediment incubation stations (1, 2, 3) in August 2013.

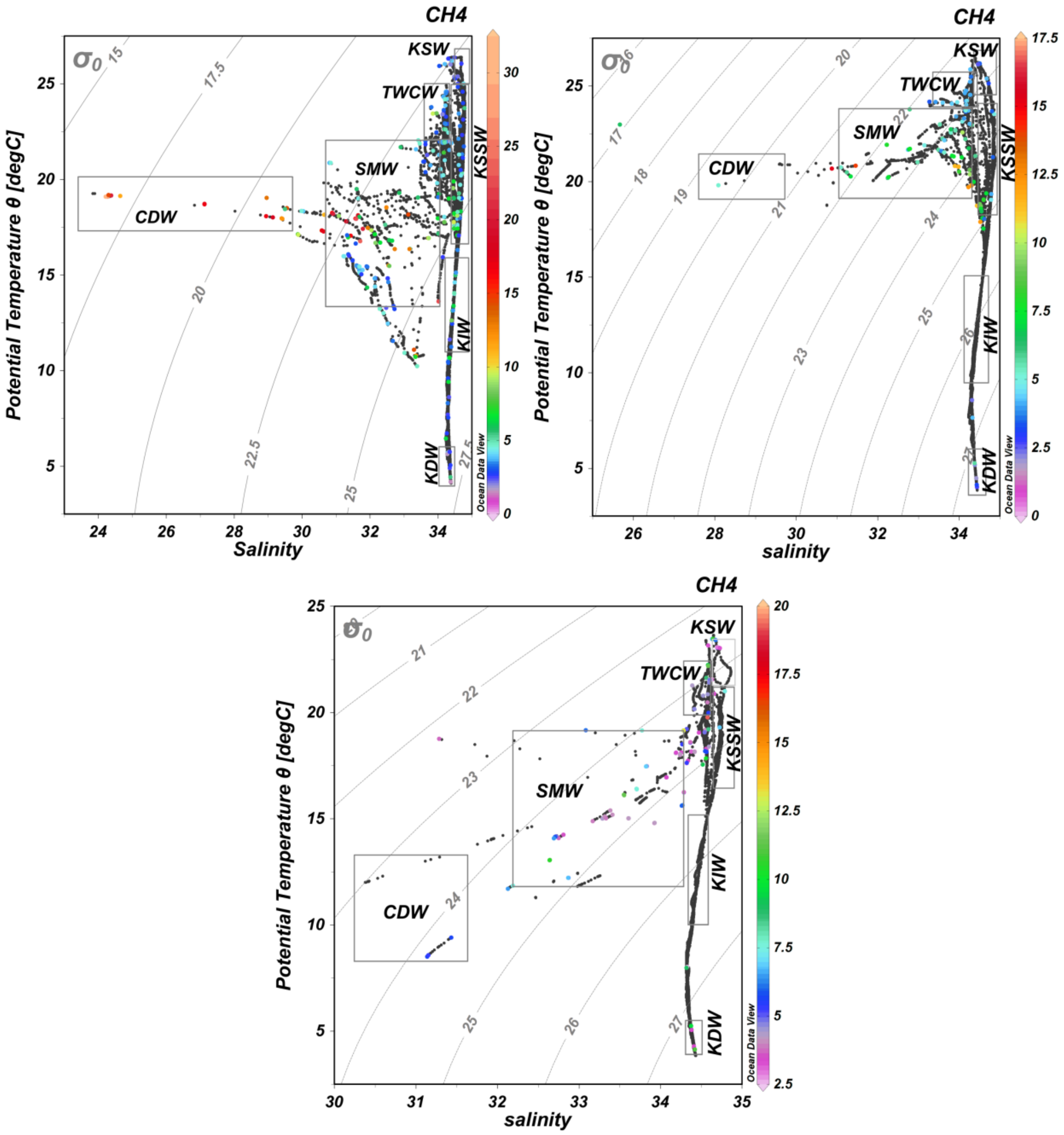

Fig. 2. Temperature-salinity diagrams and CH_4 concentrations in the East China Sea during May, October, and December of 2011. The dominant water masses are classified as previously described (Li and Su, 2000; Qi et al., 2014) and indicated by rectangular outlines. CDW: Changjiang Diluted Water; SMW: Shelf Mixed Water; KSW: Kuroshio Surface Water; KSSW: Kuroshio Subsurface Water; KIW: Kuroshio Intermediate Water; KDW: Kuroshio Deep Water; TWCW: Taiwan Warm Current Water. Black dots: non-CH_4 sampling point; Color dots: CH_4 sampling points, with concentrations indicated by color scale.

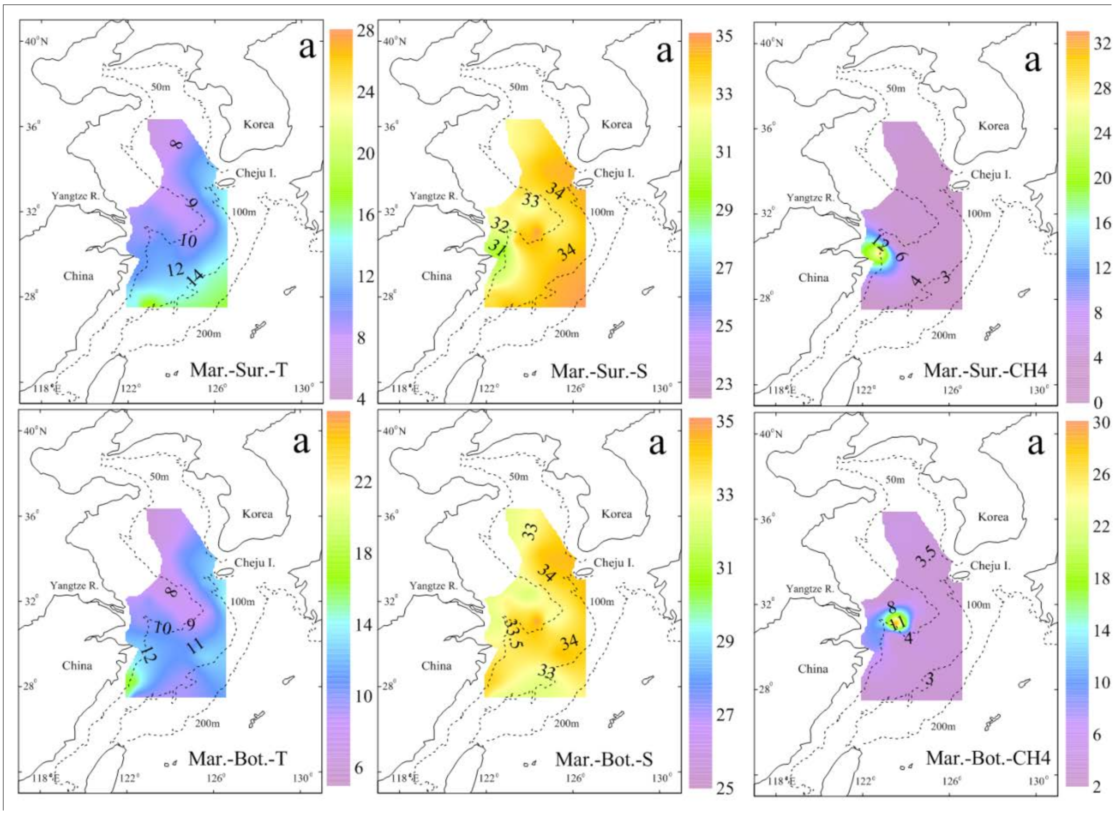
a
Mar.-Sur.-T
Mar.-Sur.-S
Mar.-Sur.-CH4
Mar.-Bot.-T
Mar.-Bot.-S
Mar.-Bot.-CH4
Korea
Cheju I.
Yangtze R.
China
50m
100m
200m
40°N
36°
32°
28°
118°E
122°
126°
130°

1

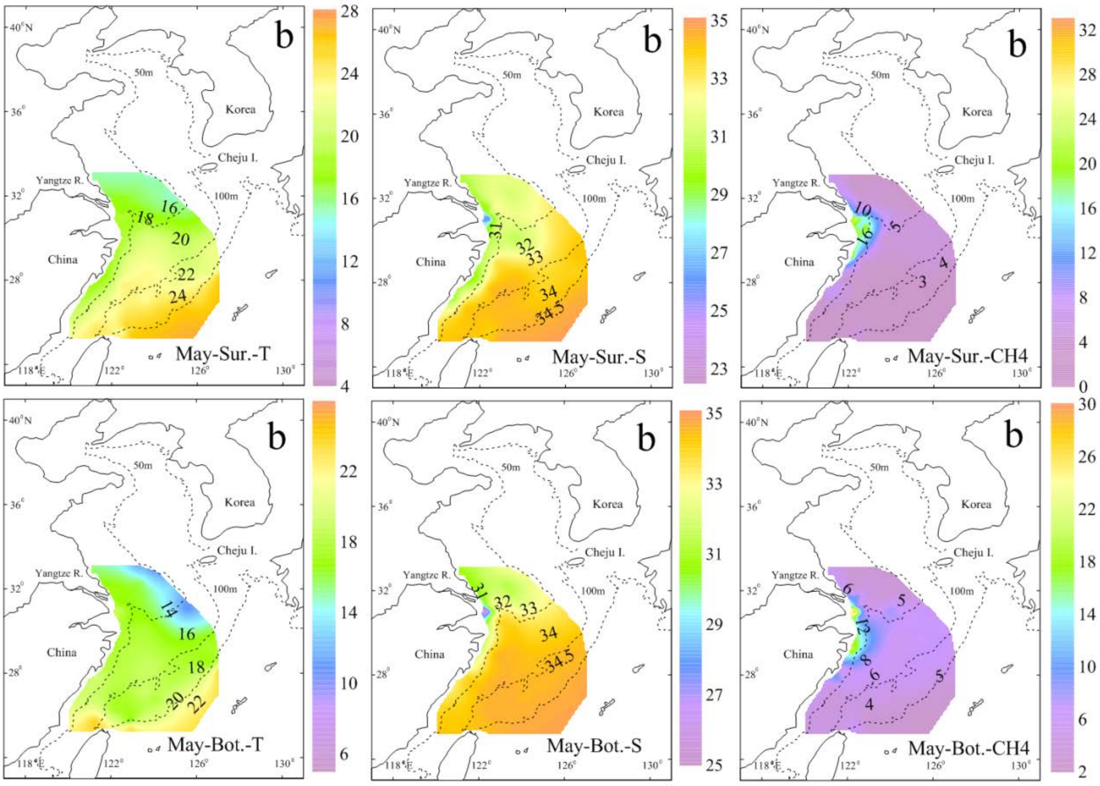
b
May-Sur.-T
May-Sur.-S
May-Sur.-CH4
May-Bot.-T
May-Bot.-S
May-Bot.-CH4
Korea
Cheju I.
Yangtze R.
China
50m
100m
40°N
36°
32°
28°
118°E
122°
126°
130°

2

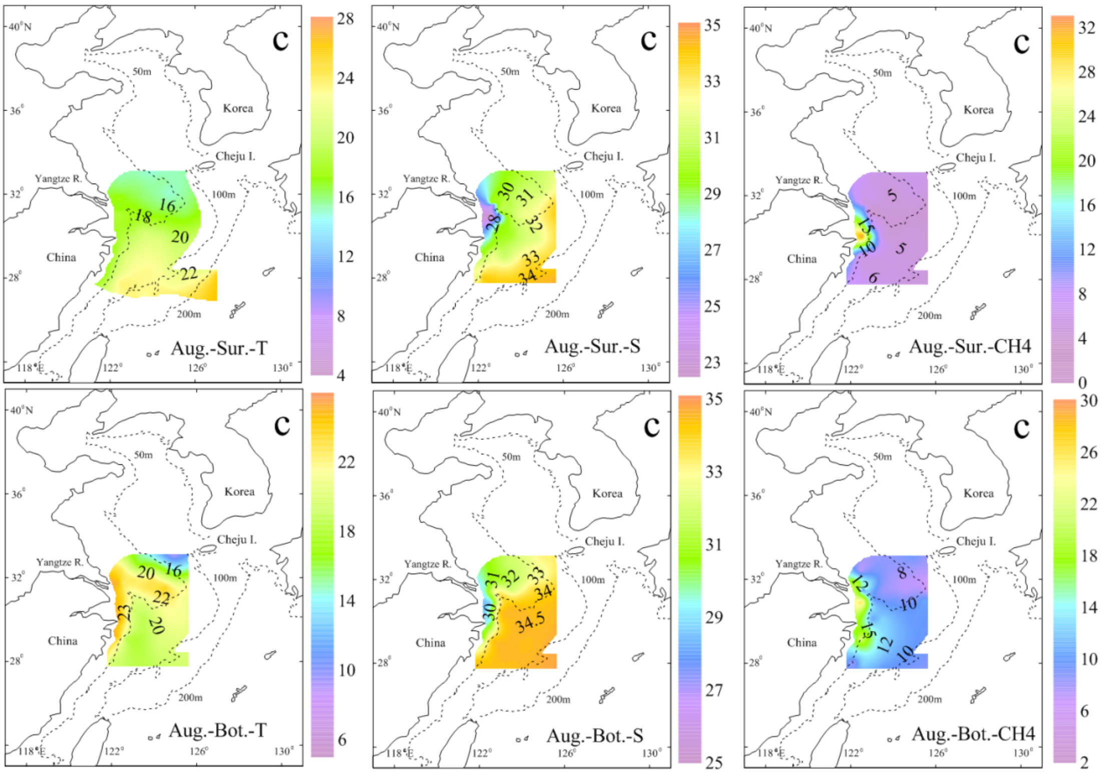
c
Aug.-Sur.-T
Aug.-Sur.-S
Aug.-Sur.-CH4
Aug.-Bot.-T
Aug.-Bot.-S
Aug.-Bot.-CH4
40°N
36°
32°
28°
118°E
122°
126°
130°
50m
100m
200m
Korea
Cheju I.
Yangtze R.
China

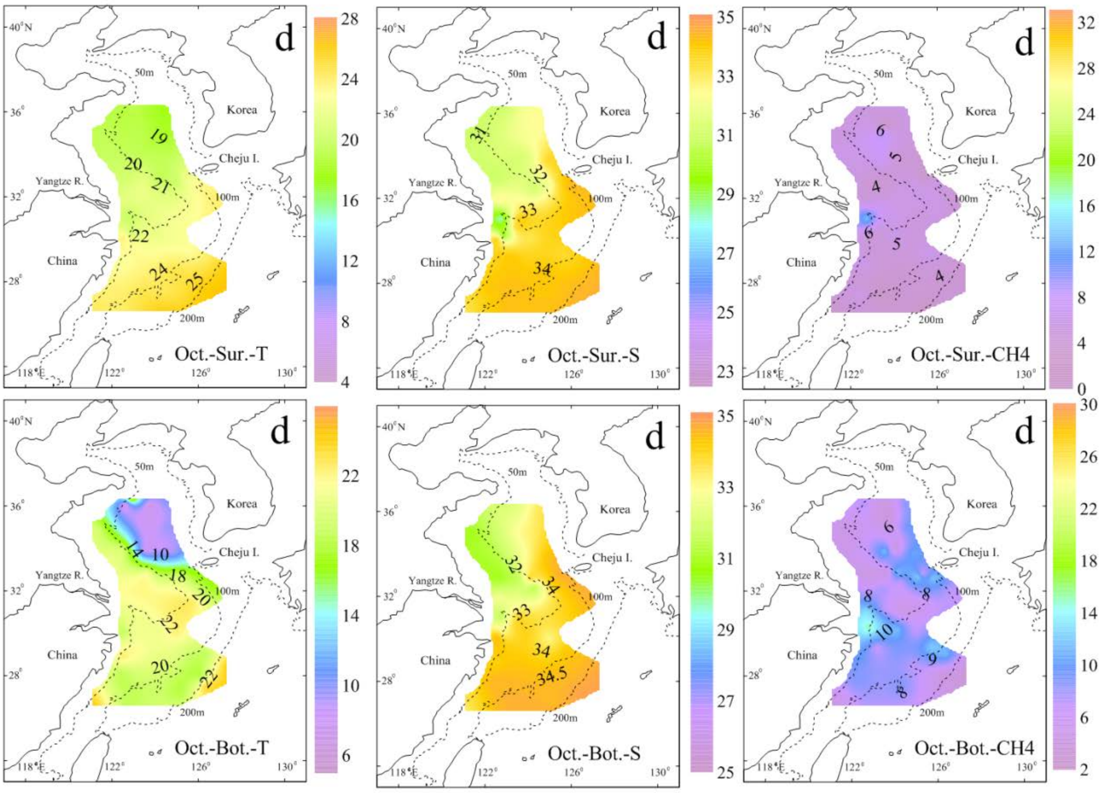
d
Oct.-Sur.-T
Oct.-Sur.-S
Oct.-Sur.-CH4
Oct.-Bot.-T
Oct.-Bot.-S
Oct.-Bot.-CH4
40°N
36°
32°
28°
118°E
122°
126°
130°
50m
100m
200m
Korea
Cheju I.
Yangtze R.
China

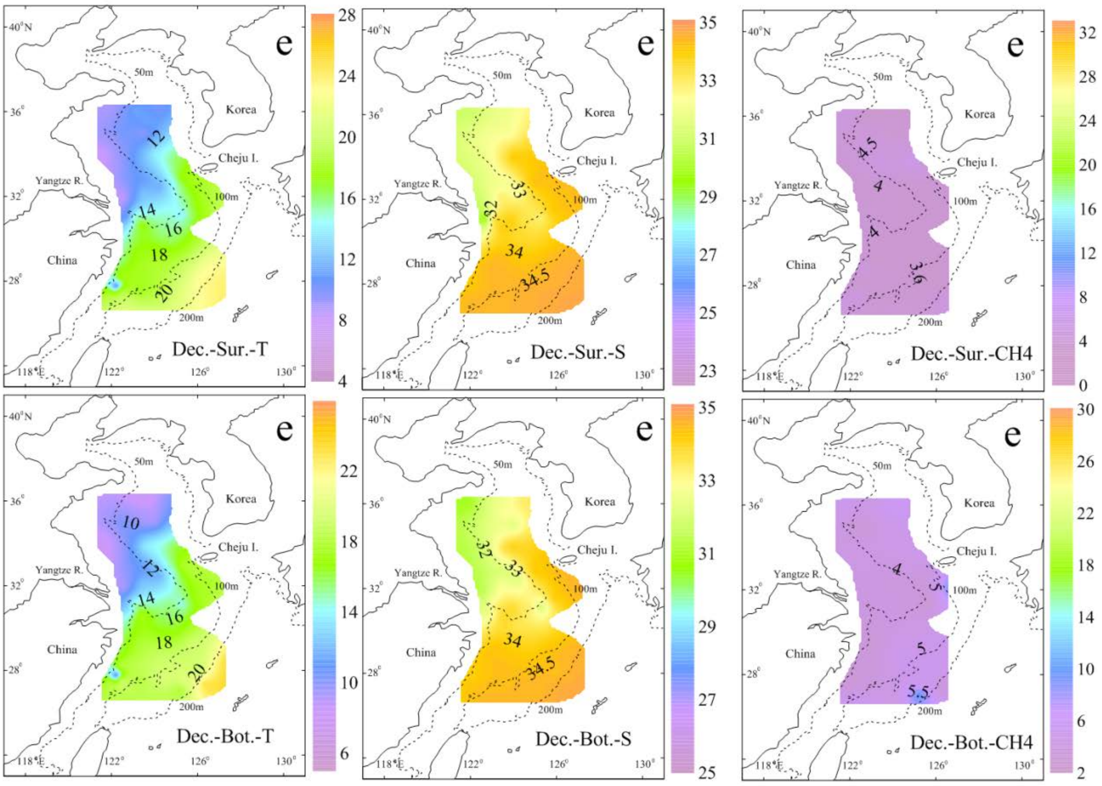

Fig. 3. Geographical distribution of temperature (°C), salinity (psu), and CH_4 (nmol·L^{-1}) in surface and bottom waters of the study area during March (a), May (b), August (c), October (d), and December (e) of 2011.

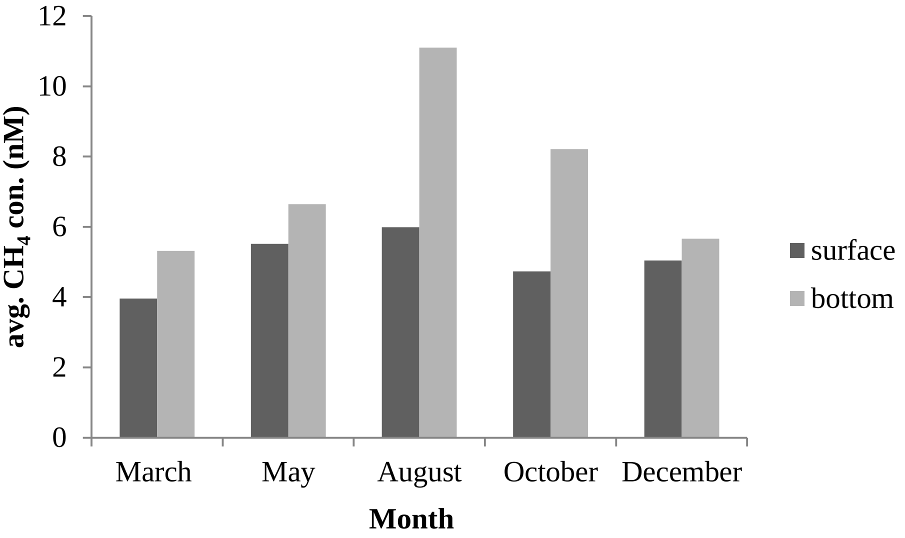

Fig. 4 Comparison of the average surface and bottom CH_4 concentrations in the ECS shelf during different seasons

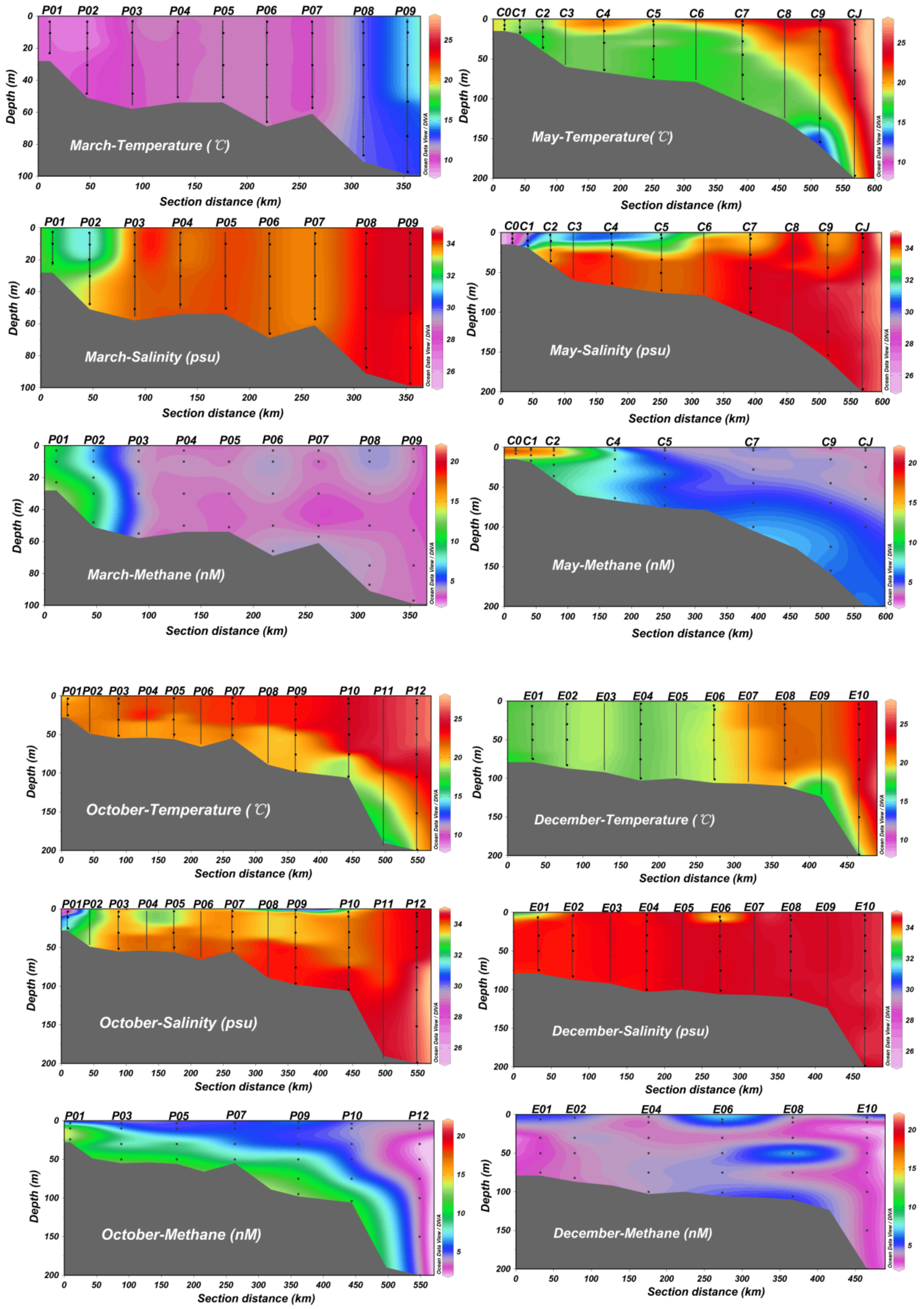

Fig. 5. Depth distributions of salinity (psu), temperature (°C), and CH_4 (nmol·L^{-1}) along section PN during March (a), May (b) and October (c) and section E during December (d).

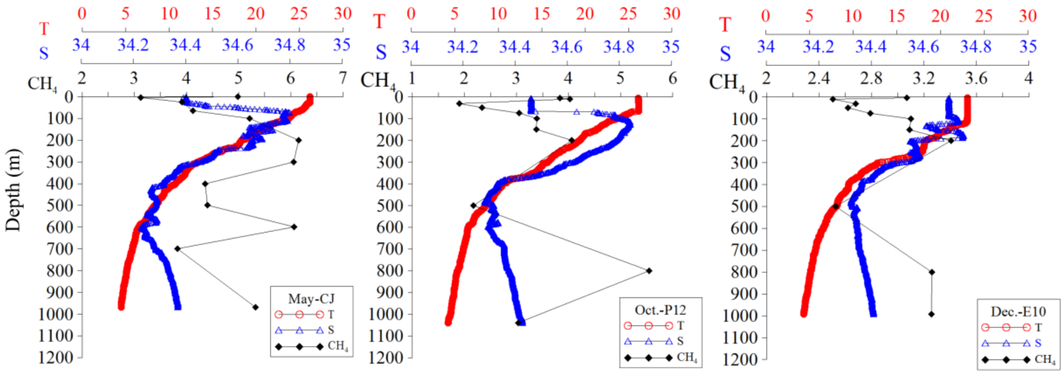

Fig. 6. Depth profiles for CH_4 ($nmol \cdot L^{-1}$), salinity (psu), and temperature (°C) at station CJ in May, station P12 in October, and station E10 in December.

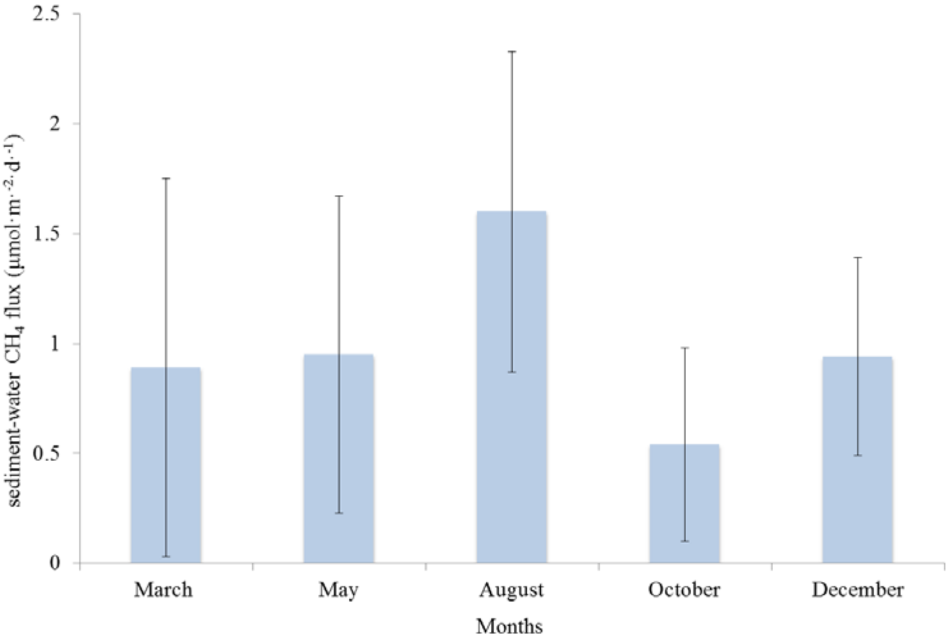

Fig. 7. Seasonal variation of sediment-water CH_4 fluxes from the East China Sea and Yellow Sea.

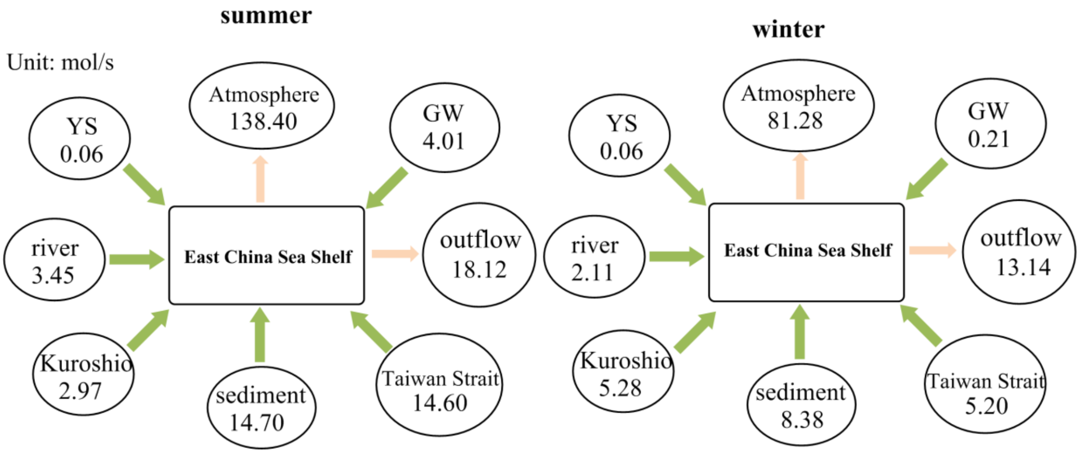

Fig. 8. CH_4 budget of the East China Sea during summer and winter.